

Joint numerical ranges of three hermitian 4×4 matrices

Piotr Pikul^a, Ilya Spitkovsky^b, Konrad Szymański^c, Stephan Weis^d,
Karol Życzkowski^{a,e}

^aJagiellonian University, Kraków, Poland

^bNew York University Abu Dhabi (NYUAD), United Arab Emirates

^cResearch Center for Quantum Information, Slovenská Akadémia Vied, Bratislava, Slovakia

^dFaculty of Electrical Engineering, Czech Technical University in Prague, Czech Republic

^eCenter for Theoretical Physics, Polish Academy of Sciences, Warsaw, Poland

Abstract

We analyze the joint numerical range W of three hermitian matrices of order four. In the generic case, this three-dimensional convex set has a smooth boundary. We analyze non-generic structures. Fifteen possible classes regarding the numbers of non-elliptic faces in the boundary of W are identified and an explicit example is presented for each class. Secondly, it is shown that a nonempty intersection of three mutually distinct one-dimensional faces is a corner point. Thirdly, introducing a tensor product structure into $\mathbb{C}^4 = \mathbb{C}^2 \otimes \mathbb{C}^2$, one defines the separable joint numerical range — a subset of W useful in studies of quantum entanglement. The boundary of the separable numerical range is compared with that of W .

Keywords: joint numerical range, hermitian matrices, convex set, face, separable numerical range, quantum states

2020 MSC: 15A60, 52A15, 47L07, 52A20

1. Introduction

The *joint numerical range* [9, p. 23] of $A_1, \dots, A_k \in M_n$, with respect to the algebra M_n of $n \times n$ matrices with complex entries, is the compact convex set

$$W := W(A_1, \dots, A_k) := \{(\operatorname{tr} \rho A_1, \dots, \operatorname{tr} \rho A_k)^\top : \rho \in M_n, \rho \geq 0, \operatorname{tr} \rho = 1\}. \quad (1.1)$$

Here, $\operatorname{tr} X$ is the trace and $X \geq 0$ means $X \in M_n$ is positive semidefinite. Equation (1.1) is a somewhat less common definition of the joint numerical range than

$$\tilde{W} := \tilde{W}(A_1, \dots, A_k) := \{\langle \varphi | A_i \varphi \rangle_{i=1}^k : |\varphi\rangle \in \mathbb{C}^n, \langle \varphi | \varphi \rangle = 1\}, \quad (1.2)$$

where $\langle \varphi_1 | \varphi_2 \rangle := \overline{x_1} y_1 + \dots + \overline{x_n} y_n$ is the inner product of $|\varphi_1\rangle = (x_1, \dots, x_n)^\top$ and $|\varphi_2\rangle = (y_1, \dots, y_n)^\top$ in \mathbb{C}^n . In any case, W is the convex hull of \tilde{W} .

Email addresses: piotr.pikul@im.uj.edu.pl (Piotr Pikul), ims2@nyu.edu (Ilya Spitkovsky), k.sz@quantumstat.es (Konrad Szymański), stephan.weis@fel.cvut.cz (Stephan Weis), karol@cft.edu.pl (Karol Życzkowski)

For a single matrix $B \in M_n$, the set $\tilde{W}(B)$ is also called *numerical range* [60, 28]. Identifying $\mathbb{C} = \mathbb{R}^2$, we have

$$\tilde{W}(B) = \tilde{W}(\operatorname{Re} B, \operatorname{Im} B), \quad (1.3)$$

as $B = \operatorname{Re} B + i \operatorname{Im} B$, where $\operatorname{Re} B := \frac{1}{2}(B + B^*)$, $\operatorname{Im} B := \frac{1}{2i}(B - B^*)$, and B^* is the hermitian conjugate of B . Similarly, $W, \tilde{W} \subset \mathbb{C}^k$ can be identified with subsets of \mathbb{R}^{2k} . Hence, unless stated otherwise, we assume A_1, \dots, A_k are hermitian. So, $W, \tilde{W} \subset \mathbb{R}^k$. It is well known that \tilde{W} is convex if $k \leq 2$ [60, 28] or if $k = 3$ and $n \geq 3$ [5, 42]. In particular, the numerical range is $W(B) = \tilde{W}(B)$, and $W(A_1, A_2, A_3) = \tilde{W}(A_1, A_2, A_3)$ holds for hermitian 4×4 matrices A_1, A_2, A_3 .

The numerical range of an operator is a well-known notion studied in operator theory and linear algebra [60, 28, 37, 18, 23, 24, 31], while its generalizations find several applications in theoretical physics [56, 38, 16, 35]. The joint numerical range is well known in matrix theory [1, 5, 8, 9, 12, 25, 39, 45, 51, 59, 61] and theoretical physics [26, 66, 58]. It is also known as the set of states [48] of a matrix system [13, 3], an algebraic object with numerous applications in quantum information theory, see for example [29, 49].

The subset W of \mathbb{R}^k has a clear interpretation in quantum physics: It is the set of possible expectation values of joint measurements of k observables A_1, \dots, A_k . The case of $k = 3$ hermitian matrices of size $n = 3$ was studied in [59], in which all possible shapes of W were divided into 10 classes with respect to the structure of its boundary. Here, we shall go beyond this case and analyze the problem of three hermitian matrices of size $n = 4$. This step forward has important consequences for quantum theory: As four is a composite number, one can introduce a tensor product structure, $\mathbb{C}^4 = \mathbb{C}^2 \otimes \mathbb{C}^2$, which corresponds to a two-qubit system. Such a splitting of a four-dimensional system into two subsystems allows for the introduction of *product states*, which convey no correlations between the two parts, and *separable states*, which encode classical correlations – all the other states are *entangled*, and among them are those whose correlations can never be explained by classical probability theory [65]. By restricting the range of states in the definition of numerical range one arrives at product [52] and separable numerical range [58], which physically correspond to classically achievable sets of expectation values. The geometry of bipartite quantum systems is also studied outside the algebraic setting of numerical ranges, see for instance [27, 40, 44, 54].

This work investigates the joint numerical range $W = W(A_1, A_2, A_3)$ of three hermitian matrices A_1, A_2, A_3 of size $n = 4$. Since $k \leq 3$, the von Neumann-Wigner non-crossing theorem implies that W is generically strictly convex and has a smooth boundary ∂W , i.e. the set of triples for which W is strictly convex and has a smooth boundary is open and dense in the set of all triples of (complex) hermitian 4×4 matrices with the Euclidean topology, see [25, Proposition 4.9] and [59, Theorem 4.2]. In the analogous sense of being true for triples of real symmetric 4×4 matrices in an open and dense set, W has generically an even number of at most ten elliptic disks

on the boundary and it has no other flat portions on ∂W . This follows from [47, Theorem 1.1], see also [30], by duality as described in Remark 6.3 below.

In this paper we focus on non-elliptic flat portions on ∂W . Any flat portion on ∂W corresponds to the numerical range of a 3×3 matrix B , see Remark 2.3 (c), (d) for details. The classification of these numerical ranges was achieved by Kippenhahn [37]. See also [36, 20] and, for more rigorous proofs, see [12, 51]. Let

$$p_B(u_0, u_1, u_2) := \det(u_0 \mathbf{1}_3 + u_1 \operatorname{Re} B + u_2 \operatorname{Im} B), \quad u_0, u_1, u_2 \in \mathbb{C}, \quad (1.4)$$

and let $C(B)$ be the dual curve [19] to the curve $p_B = 0$ that consists of all tangent lines to $p_B = 0$. Identifying the complex projective plane $\mathbb{C}\mathbb{P}^2$ with its dual space of lines, we define $C_{\mathbb{R}}(B) := \{(x_1, x_2)^{\top} \in \mathbb{R}^2 \mid (1 : x_1 : x_2) \in C(B)\}$. The set $C_{\mathbb{R}}(B)$ is known as the *Kippenhahn curve* [6, 20] and $\tilde{W}(B)$ is the convex hull of $C_{\mathbb{R}}(B)$. This result divides the shape of $\tilde{W}(B)$ into four different classes [20]:

1. $C_{\mathbb{R}}(B)$ consists of three points that are the eigenvalues of B , and $\tilde{W}(B)$ is the closed triangular region whose vertices are these points.
2. $C_{\mathbb{R}}(B)$ consists of an ellipse and a point. Depending on whether the point lies inside the ellipse or not, $\tilde{W}(B)$ is an elliptic disk or it has a *droplet shape*.
3. $C(B)$ is an irreducible curve of degree four that has a double tangent, $C_{\mathbb{R}}(B)$ is of heart shape, and the boundary of $\tilde{W}(B)$ contains a line segment but no corner.
4. $C(B)$ is an irreducible curve of degree six, $C_{\mathbb{R}}(B)$ consists of two parts, one inside the other. The outer part is an oval (a smooth and strictly convex curve), whose convex hull is $\tilde{W}(B)$.

For simplicity (see Lemma 3.1 and Example 3.3) we focus on flat parts of the boundary ∂W different from elliptic disks. This prompts the following definitions.

A *face* of a convex subset C of \mathbb{R}^d is a convex subset of C that contains the endpoints $x, y \in C$ of every open segment $\{(1 - \lambda)x + \lambda y : \lambda \in (0, 1)\}$ it intersects. An *exposed face* of C is the set of minimizers of any linear functional on C . For technical reasons, \emptyset is also considered an exposed face. It is well known that every exposed face of C is a face of C . Faces that are not exposed faces are called *nonexposed faces* [53].

Definition 1.1 (Non-elliptic faces). Let A_1, A_2, A_3 be hermitian 4×4 matrices such that $W = W(A_1, A_2, A_3)$ has dimension $\dim(W) = 3$. A *non-elliptic face* of W is any two-dimensional face of W that is not an elliptic disc. We say a non-elliptic face of W has *type* $m \in \{0, 1, 2, 3\}$ if it has m one-dimensional faces.

¹Note that the image scalings are not proportional (aspect ratios differ from one). Having a double eigenvalue at its coinciding foci, the ellipse in the third drawing depicts a circle.

type	shape	Kippenhahn curve
0	oval	degree-6 curve
1	loaf	degree-4 curve
2	droplet	ellipse and a point outside the ellipse
3	triangle	three affinely independent points

Table 1: The four types and shapes of non-elliptic faces and their Kippenhahn curves.

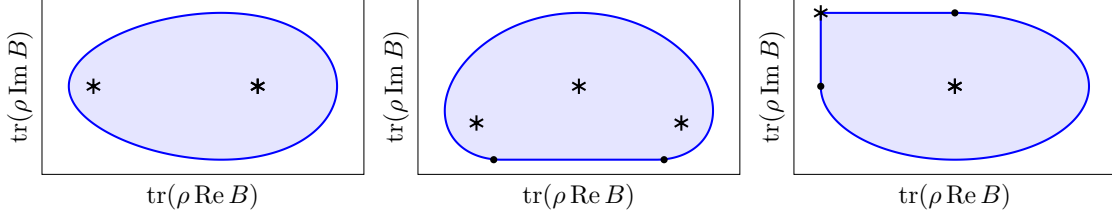


Figure 1.1: Examples of numerical ranges of a 3×3 matrix B in the complex plane exemplifying the shapes of type 0 (oval), 1 (loaf) and 2 (droplet). Black asterisks mark the (in some cases, duplicate) eigenvalues¹ of B . Small black dots mark the nonexposed faces of the numerical ranges — endpoints of segments smoothly connected to the rest of the boundary. The missing numerical range of type 3 is a triangle, which is the convex hull of the three eigenvalues of a normal matrix, $BB^* = B^*B$.

Non-elliptic faces being numerical ranges of 3×3 matrices, each type 0, 1, 2, and 3 refers to a unique shape in Kippenhahn’s classification above, see Table 1. Exemplary matrices for each type read,

$$\begin{bmatrix} -1 & 1 & 1 \\ 0 & \frac{1}{2} & 1 \\ 0 & 0 & \frac{1}{2} \end{bmatrix}, \quad \frac{1}{2} \begin{bmatrix} 1 & 0 & -i \\ 0 & -1 & -i \\ i & i & 2i \end{bmatrix}, \quad \begin{bmatrix} 1 & 2 & 0 \\ 0 & 1 & 0 \\ 0 & 0 & i \end{bmatrix}, \quad \begin{bmatrix} -1 & 0 & 0 \\ 0 & 1 & 0 \\ 0 & 0 & i \end{bmatrix}.$$

The numerical ranges for the first three of the above matrices of type 0, 1 and 2, are depicted in Figure 1.1. The numerical range of the diagonal matrix of type 3 is the convex hull of the eigenvalues: The triangle with vertices at $-1, 1$ and i .

We continue the paper by recalling and proving preliminaries on the algebra and geometry of the joint numerical range in Section 2. Section 3 contains one of the main results of the paper, Theorem 3.6, which establishes 15 classes that capture all possible numbers of non-elliptic face of the joint numerical range W of three hermitian 4×4 matrices. Section 4 presents an example of W for every class. A second major result is Theorem 5.10 of Section 5, according to which a non-empty intersection of three mutually distinct one-dimensional faces of W is a corner point of W . Section 6 collects observations and examples regarding ellipses on the boundary of W that motivated us to initiate this work. In Section 7, we compare the structure of the standard joint numerical range W with the separable numerical range.

2. Algebra and geometry of the joint numerical range

Summarizing prior work of one of the authors [61, 62], this section presents an algebraic description of the faces of the joint numerical range. Normal cones are reviewed, too, and properties of corner points are discussed, including the assertion proved by Binding and Li [8] that every corner point of the joint numerical range is contained in the joint spectrum. Bonsall and Duncan's notion of the joint numerical range with respect to a $*$ -algebra [9] is convenient for the analysis of faces.

The algebra M_n of $n \times n$ complex matrices is a unitary space with the Frobenius inner product $\langle A, B \rangle := \text{tr}(A^*B)$, $A, B \in M_n$. It is a $*$ -algebra with the involution $A \mapsto A^*$ mapping a matrix $A \in M_n$ to its conjugate transpose. The algebra M_n is partially ordered by $A \leq B$, or equivalently $B \geq A$, meaning that $B - A$ is positive semidefinite. Let $\mathbb{1}_n$ be the $n \times n$ identity matrix. We define a $*$ -algebra on \mathbb{C}^n to be a complex linear subspace of M_n that is closed under matrix multiplication and under the involution $A \mapsto A^*$.

Let \mathcal{A} be a $*$ -algebra on \mathbb{C}^n , $\mathcal{H}_{\mathcal{A}} := \{A \in \mathcal{A} : A^* = A\}$ be the real vector space of hermitian matrices, and let $A_1, \dots, A_k \in \mathcal{H}_{\mathcal{A}}$. Let also

$$w = w_{A_1, \dots, A_k} : \mathcal{H}_{\mathcal{A}} \rightarrow \mathbb{R}^k, \quad w(A) := (\langle A, A_1 \rangle, \dots, \langle A, A_k \rangle)^\top. \quad (2.1)$$

The image of the set of *density matrices*

$$\mathcal{D}_{\mathcal{A}} := \{\rho \in \mathcal{A} : \rho \geq 0 \text{ and } \text{tr}(\rho) = 1\} \quad (2.2)$$

under w is the *joint numerical range*² of A_1, \dots, A_k with respect to the $*$ -algebra \mathcal{A} , which we denote by

$$W_{\mathcal{A}}(A_1, \dots, A_k) := w(\mathcal{D}_{\mathcal{A}}), \quad (2.3)$$

see [9, Definition 11]. We are mostly interested in the joint numerical range

$$W_{M_n}(A_1, \dots, A_k) = \{(\text{tr } \rho A_1, \dots, \text{tr } \rho A_k)^\top : \rho \in M_n, \rho \geq 0, \text{tr } \rho = 1\}, \quad (2.4)$$

with respect to the full matrix algebra M_n , which we also denote by $W(A_1, \dots, A_k)$ or simply by W . The set W is also known as the ‘‘algebraic numerical range’’ [45].

It is well known [2] that there is an isomorphism between the set of exposed faces of $\mathcal{D}_{\mathcal{A}}$ and the set $\mathcal{P}_{\mathcal{A}} := \{P \in \mathcal{A} : P = P^2 = P^*\}$ of orthogonal projections. Namely, if $A \in \mathcal{A}$ is a hermitian matrix, then the set of minimizers of the real affine functional $\mathcal{D}_{\mathcal{A}} \rightarrow \mathbb{R}$, $\rho \mapsto \langle \rho, A \rangle$ is the set \mathcal{D}_{PAP} of density matrices of the $*$ -algebra PAP , where P is the spectral projection of A in the $*$ -algebra \mathcal{A} corresponding to the smallest spectral value³ of A with respect to \mathcal{A} . The map $P \mapsto \mathcal{D}_{PAP}$ is a lattice

²To be precise, the joint numerical range is defined in [9] in terms of states on the algebra \mathcal{A} , that is to say, normalized positive linear functionals. This is equivalent to the aforementioned definition because states are represented by density matrices, see the Sections 2.3.2 and 2.4.3 in [10].

³The use of spectral values (as opposed to eigenvalues) is mandatory, because the identity Q of the $*$ -algebra QM_nQ differs from $\mathbb{1}_n$ for every $n \times n$ orthogonal projection $Q \neq \mathbb{1}_n$. Spectral values were introduced into this finite-dimensional setting in the arXiv-version of [61], see also the erratum to [61].

isomorphism from $\mathcal{P}_{\mathcal{A}}$ to the set of exposed faces of $\mathcal{D}_{\mathcal{A}}$. Thereby, $\mathcal{P}_{\mathcal{A}}$ is partially ordered by $P \leq Q$ (the range of P is a subset of the range of Q). The set $\mathcal{P}_{\mathcal{A}}$ is a complete lattice in this partial order, which means any subset of $\mathcal{P}_{\mathcal{A}}$ has an infimum and a supremum. The set of exposed faces is partially ordered by inclusion and the infimum is the intersection.

A similar isomorphism exists between the faces of the joint numerical range and certain orthogonal projections [61]. However, whereas all faces of $\mathcal{D}_{\mathcal{A}}$ are exposed faces, the joint numerical range W can have nonexposed faces. Fig. 1.1 shows examples: the endpoints of flat portions on the boundary of the numerical range that are joined by curved boundary portions. Two ideas suffice to describe the faces of the joint numerical range. First, as with exposed faces, the set of faces of a convex subset C of a Euclidean space, partially ordered by inclusion, is a complete lattice, whose infimum is the intersection [41, 62]. Second, we define an *access sequence*⁴ [22, 14] of faces (of length ℓ) with respect to C to be a nonincreasing sequence

$$F_0 \supset F_1 \supset \cdots \supset F_\ell \quad (2.5)$$

subject to the conditions that $F_0 = C$, that F_{i+1} is an exposed face of F_i , $i = 0, \dots, \ell - 1$, and that $F_\ell \neq \emptyset$. Clearly [62, Section 1.2.1], a nonempty subset F of C is a face of C if and only if F is an element of an access sequence with respect to C . This follows from a separation argument [62, Lemma 4.6] proving that every face of C that is strictly included in C is included in an exposed face of C that is itself strictly included in C .

The set of hermitian matrices, density matrices, and orthogonal projections in M_n is denoted by $\mathcal{H}_n := \mathcal{H}_{M_n}$, $\mathcal{D}_n := \mathcal{D}_{M_n}$ and $\mathcal{P}_n := \mathcal{P}_{M_n}$, respectively. Let $A_1, \dots, A_k \in \mathcal{H}_n$ denote arbitrary hermitian $n \times n$ matrices. The $*$ -algebra

$$PM_nP = \{PAP : A \in M_n\}$$

is defined in terms of a nonzero orthogonal projection $P \in \mathcal{P}_n$. An *access sequence* of projections (of length ℓ) with respect to A_1, \dots, A_k is a nonincreasing sequence

$$P_0 \geq P_1 \geq \cdots \geq P_\ell \quad (2.6)$$

of orthogonal projections in \mathcal{P}_n , subject to the conditions that $P_0 = \mathbb{1}_n$ and that for every $i = 0, \dots, \ell - 1$ there exists a tuple of real numbers $s_1, \dots, s_k \in \mathbb{R}$ such that P_{i+1} is the spectral projection of $P_i(s_1A_1 + \cdots + s_kA_k)P_i$ in the $*$ -algebra $P_iM_nP_i$ corresponding to the smallest spectral value of $P_i(s_1A_1 + \cdots + s_kA_k)P_i$ with respect to $P_iM_nP_i$.

It is easy to see that W is affinely isomorphic to an orthogonal projection of \mathcal{D}_n . Let $\pi_{\mathcal{U}} : \mathcal{H}_n \rightarrow \mathcal{H}_n$ denote the orthogonal projection onto a subspace \mathcal{U} of \mathcal{H}_n . If \mathcal{U}

⁴An element of an access sequence with respect to a convex set has been called a *poonem* in convex geometry [22]. The term *access sequence* stems from mathematical statistics [14].

is the real linear span of A_1, \dots, A_k , then $w_{A_1, \dots, A_k} : \mathcal{H}_n \rightarrow \mathbb{R}^k$ restricts to the affinity

$$w_{A_1, \dots, A_k} : \pi_{\mathcal{U}}(\mathcal{D}_n) \rightarrow W \quad (2.7)$$

(see [61, Remark 1.1] for details). Similarly, $w_{\mathbb{1}_n, A_1, \dots, A_k} : \mathcal{H}_n \rightarrow \mathbb{R}^{k+1}$ restricts to the affinity

$$w_{\mathbb{1}_n, A_1, \dots, A_k} : \pi_{\mathcal{V}}(\mathcal{D}_n) \rightarrow \{1\} \times W \quad (2.8)$$

if $\mathcal{V} = \text{span}\{\mathbb{1}_n, A_1, \dots, A_k\}$, because $\text{tr } \rho = 1$ holds for every $\rho \in \mathcal{D}_n$. The following theorem follows from [61, Theorem 3.7] through a family of affinities of the type (2.7). More details can be found in [63, Section 4.1], in particular in Lemma 4.19 therein.

Theorem 2.1. *There is a one-to-one correspondence between access sequences of orthogonal projections $P_0 \geq P_1 \geq \dots \geq P_\ell$ with respect to A_1, \dots, A_k and access sequences of faces $F_0 \supset F_1 \supset \dots \supset F_\ell$ with respect to W . For every $i = 0, \dots, \ell$ we have $F_i = w(\mathcal{D}_{P_i M_n P_i})$ and $P_i \in \mathcal{P}_n$ is the unique orthogonal projection such that $\mathcal{D}_{P_i M_n P_i} = w|_{\mathcal{D}_n}^{-1}(F_i)$.*

By Theorem 2.1, for every nonempty face F of W there is a unique orthogonal projection $P \in \mathcal{P}_n$ that satisfies $\mathcal{D}_{P M_n P} = w|_{\mathcal{D}_n}^{-1}(F)$. We call P the *projection associated to F* and refer to F as a *rank- r face* of W if $r = \text{rk}(P)$.

Example 2.2. Let $k = 3$, let $W = W(A_1, A_2, A_3)$ be the joint numerical range of three hermitian 4×4 matrices A_1, A_2, A_3 , and assume $\dim(W) = 3$. Let F_1 be a non-elliptic face of W , F_2 a one-dimensional face of F_1 , and p an endpoint of the segment F_2 . After applying to A_1, A_2, A_3 the similarity $A \mapsto UAU^*$ with respect to a suitable unitary $U \in M_4$, the access sequence of projections $\mathbb{1}_4 \geq P_1 \geq P_2 \geq P_3$ that corresponds to the access sequence of faces $W \supset F_1 \supset F_2 \supset \{p\}$ by Theorem 2.1 is $P_1 = \text{diag}(1, 1, 1, 0)$, $P_2 = \text{diag}(1, 1, 0, 0)$, and $P_3 = \text{diag}(1, 0, 0, 0)$.

We show in Remark 2.3 that every rank- r face F of W is the joint numerical range of k hermitian $r \times r$ matrices and that F is isometric to the joint numerical range of $d = \dim(F)$ hermitian $r \times r$ matrices. To this end, we employ the leading principal submatrix $A[r]$ of a matrix $A \in M_n$ obtained by deleting the rows and columns $r + 1$ through n .

Note that $F = w(\mathcal{D}_{P M_n P})$ holds for every face F of W and the projection P associated to F by Theorem 2.1. In general, for arbitrary nonzero $P \in \mathcal{P}_n$, the set $w(\mathcal{D}_{P M_n P})$ is not a face of W but it is still useful in Lemma 2.6 and Corollary 2.7.

Remark 2.3. Let $P \in \mathcal{P}_n$ be a projection of rank $r > 0$, and let $F := w(\mathcal{D}_{P M_n P})$. Then:

- (a) As per the definition in equation (2.3), the convex set F is a joint numerical range:

$$\begin{aligned} F &= \{\langle \rho, A_i \rangle_{i=1}^k : \rho \in \mathcal{D}_{P M_n P}\} = \{\langle \rho, P A_i P \rangle_{i=1}^k : \rho \in \mathcal{D}_{P M_n P}\} \\ &= W_{P M_n P}(P A_1 P, \dots, P A_k P) \end{aligned}$$

- (b) The matrix size n can be decreased at the expense of a unitary similarity. Let U be a unitary $n \times n$ matrix such that $Q := UPU^*$ has the block diagonal form $Q = \mathbb{1}_r \oplus 0$. The matrix PAP is unitarily similar to $UPAPU^* = QUAU^*Q = UAU^*[r] \oplus 0$ for every $A \in M_n$. Moreover, the trace-preserving *-algebra isomorphism

$$PM_nP \rightarrow M_r, \quad A \mapsto (UAU^*)[r]$$

restricts to an isometry $\mathcal{D}_{PM_nP} \rightarrow \mathcal{D}_{M_r}$. Hence,

$$\begin{aligned} F &= \{\langle \rho, PA_iP \rangle_{i=1}^k : \rho \in \mathcal{D}_{PM_nP}\} = \{\langle U\rho U^*[r], UA_iU^*[r] \rangle_{i=1}^k : \rho \in \mathcal{D}_{PM_nP}\} \\ &= \{\langle \sigma, UA_iU^*[r] \rangle_{i=1}^k : \sigma \in \mathcal{D}_{M_r}\} = W((UA_1U^*)[r], \dots, (UA_kU^*)[r]). \end{aligned}$$

- (c) The number k of matrices can be reduced to the dimension $d = \dim(F)$ of F at the cost of an affine transformation with coefficients $t_{ij} \in \mathbb{R}$, $i = 1, \dots, l$, $j = 0, \dots, k$,

$$T : \mathbb{R}^k \rightarrow \mathbb{R}^l, \quad (x_1, \dots, x_k)^\top \mapsto (t_{i0} + \sum_{j=1}^k t_{ij}x_j)_{i=1}^l. \quad (2.9)$$

Let

$$\hat{A}_i := t_{i0}\mathbb{1}_n + \sum_{j=1}^k t_{ij}A_j, \quad i = 1, \dots, l. \quad (2.10)$$

Then for every $\rho \in \mathcal{D}_n$ we have

$$T \circ w_{A_1, \dots, A_k}(\rho) = w_{\hat{A}_1, \dots, \hat{A}_l}(\rho). \quad (2.11)$$

In particular, $T(W) = W(\hat{A}_1, \dots, \hat{A}_l)$. Let $T : \mathbb{R}^k \rightarrow \mathbb{R}^l$ be a rotation such that for every $i = d+1, \dots, k$ the number $\langle \rho, \hat{A}_i \rangle = c_i$ is constant for all $\rho \in \mathcal{D}_{PM_nP}$. Then

$$\begin{aligned} T(F) &= \{\langle \rho, \hat{A}_i \rangle_{i=1}^k : \rho \in \mathcal{D}_{PM_nP}\} = \{\langle \rho, \hat{A}_i \rangle_{i=1}^d : \rho \in \mathcal{D}_{PM_nP}\} \times \{c\} \\ &= W((U\hat{A}_1U^*)[r], \dots, (U\hat{A}_dU^*)[r]) \times \{c\}, \end{aligned} \quad (2.12)$$

where $c = (c_{d+1}, \dots, c_k)^\top$ and U is the unitary from part (b) above. Hence, F is isometric to the joint numerical range $W((U\hat{A}_1U^*)[r], \dots, (U\hat{A}_dU^*)[r])$.

- (d) It often suffices to study F though an affinity rather than an isometry. Let \mathcal{V} be the linear span of the matrices $\mathbb{1}_r, (UA_1U^*)[r], \dots, (UA_kU^*)[r]$ introduced in part (b) above and let $B_1, \dots, B_l \in \mathcal{H}_r$ satisfy

$$\text{span}\{\mathbb{1}_r, B_1, \dots, B_l\} = \mathcal{V}.$$

Then the joint numerical ranges F and $W(B_1, \dots, B_l)$ are affinely isomorphic. Indeed, by part (b) above we have $F = W((UA_1U^*)[r], \dots, (UA_kU^*)[r])$ and the maps

$$\begin{aligned} w_{\mathbb{1}_r, (UA_1U^*)[r], \dots, (UA_kU^*)[r]} : \pi_{\mathcal{V}}(\mathcal{D}_r) &\rightarrow \{1\} \times W((UA_1U^*)[r], \dots, (UA_kU^*)[r]) \\ w_{\mathbb{1}_r, B_1, \dots, B_l} : \pi_{\mathcal{V}}(\mathcal{D}_r) &\rightarrow \{1\} \times W(B_1, \dots, B_l) \end{aligned}$$

are affinities by equation (2.8).

Let C be a convex subset of a Euclidean space E . The *normal cone* of C at $x \in C$ is the closed convex cone

$$N_C(x) := \{u \in E \mid \forall y \in C: \langle y - x, u \rangle \geq 0\}.$$

We put $N_C(\emptyset) := E$. The *normal cone* of C at a nonempty convex subset G of C is

$$N_C(G) := \bigcap_{x \in G} N_C(x).$$

Note that $N_C(G) = N_C(x)$ holds for every point x in the relative interior⁵ of G , see [62, Definition 4.3]. The set of *normal cones* of C is defined as $\{N_C(G) : G \subset C \text{ is convex}\}$.

By [62, Propositions 4.7 and 4.8] we have the following.

Proposition 2.4. *The set of normal cones of a convex subset C of a Euclidean space E is a complete lattice with respect to the partial order by inclusion. If $K \subset L \neq E$ are normal cones of C , then K is a face of L . If C is not a singleton, then $F \mapsto N_C(F)$ is an antitone lattice isomorphism from the set of exposed faces to the set of normal cones of C .*

A point $x \in C$ is a *corner point* of C if $N_C(x)$ has full dimension $\dim(N_C(x)) = \dim(E)$. It is well known, see [8, Proposition 2.5], that every corner point $p = (p_1, \dots, p_k)^\top \in \mathbb{R}^k$ of W is contained in the *joint spectrum*

$$\{(\lambda_1, \dots, \lambda_k)^\top \in \mathbb{R}^k \mid \exists |\varphi\rangle \in \mathbb{C}^n \setminus \{0\}, \forall i = 1, \dots, k: A_i |\varphi\rangle = \lambda_i |\varphi\rangle\}$$

of the hermitian matrices $A_1, \dots, A_k \in M_n$. This shows that there is a nonzero $|\varphi\rangle \in \mathbb{C}^n$ such that $A_i |\varphi\rangle = A_i^* |\varphi\rangle = p_i |\varphi\rangle$, $i = 1, \dots, k$, which means that $|\varphi\rangle$ is a *normal eigenvector* of A_i , $i = 1, \dots, k$. Hence [31, p. 123], there is a unitary $n \times n$ matrix U , such that

$$UA_iU^* = p_i \oplus B_i = \begin{bmatrix} p_i & 0 \\ 0 & B_i \end{bmatrix}, \quad i = 1, \dots, k$$

for certain hermitian $(n-1) \times (n-1)$ matrices B_1, \dots, B_k . We arrive at the same conclusion in Proposition 2.5. Let $\mathbb{C}\mathbf{1}_n := \{z\mathbf{1}_n \mid z \in \mathbb{C}\}$ and

$$\begin{aligned} \mathbb{C}P \oplus P'M_nP' &:= \{zP + P'AP' \mid z \in \mathbb{C}, A \in M_n\}, \\ PM_nP \oplus P'M_nP' &:= \{PAP + P'AP' \mid A \in M_n\}, \end{aligned}$$

for every orthogonal projection $P \in \mathcal{P}_n$, $P \neq 0, \mathbf{1}_n$, where $P' := \mathbf{1}_n - P$.

Proposition 2.5. *Let p be a corner point of W and let $P \in \mathcal{P}_n$ be the projection associated to $\{p\}$. If $P = \mathbf{1}_n$, then $A_1, \dots, A_k \in \mathbb{C}\mathbf{1}_n$. Otherwise $A_1, \dots, A_k \in \mathbb{C}P \oplus P'M_nP'$.*

⁵The *relative interior* [53] of a convex set C is the interior of C in the topology of its affine hull.

Proof. We replace W with the projection $\mathcal{C} := \pi_{\mathcal{V}}(\mathcal{D}_n)$ of \mathcal{D}_n onto the span \mathcal{V} of $\mathbb{1}_n, A_1, \dots, A_k$. The map $w_{\mathbb{1}_n, A_1, \dots, A_k} : \mathcal{H}_n \rightarrow \mathbb{R}^{k+1}$ restricts to the affinity $w_{\mathbb{1}_n, A_1, \dots, A_k} : \mathcal{C} \rightarrow \{1\} \times W$ by equation (2.8). The matrix $M := w|_{\mathcal{C}}^{-1}(1, p)$ is therefore a corner point of \mathcal{C} . Since M is an exposed point of \mathcal{C} , equations (3.10) and (4.5) in [64] show that the normal cone of \mathcal{C} at M in \mathcal{V} is

$$N_{\mathcal{C}}(M) = \{A \in \mathcal{H}_n \mid P \leq P_-(A)\} \cap \mathcal{V},$$

where $P_-(A)$ is the spectral projection of $A \in \mathcal{H}_n$ corresponding to the smallest eigenvalue. As shown in [64], formula (5.3), we have

$$N_{\mathcal{C}}(M) = \mathbb{R}\mathbb{1}_n + (P'M_n^+P' \cap \mathcal{V}),$$

where M_n^+ denotes the cone of positive semidefinite $n \times n$ matrices. Since M is a corner point, \mathcal{V} is included in the linear span of $N_{\mathcal{C}}(M)$. This shows that $\mathcal{V} \subset \mathbb{R}\mathbb{1}_n + (P'\mathcal{H}_nP')$ and proves the claim. \square

The next lemma describes the joint numerical range of a reducible tuple of hermitian matrices. We skip its straightforward proof.

Lemma 2.6. *Let $P \in \mathcal{P}_n$, $P \neq 0, \mathbb{1}_n$, and let $A_1, \dots, A_k \in PM_nP \oplus P'M_nP'$. Then*

$$W = \text{conv}[W_{PM_nP}(PA_1P, \dots, PA_kP) \cup W_{P'M_nP'}(P'A_1P', \dots, P'A_kP')].$$

If, in addition, $p := (p_1, \dots, p_k)^\top \in \mathbb{R}^k$, and $A_iP = p_iP$, $i = 1, \dots, k$, then

$$W = \text{conv}[\{p\} \cup W_{P'M_nP'}(P'A_1P', \dots, P'A_kP')].$$

Corollary 2.7. *Assume that W is not a singleton and let p be a corner point of W . Then W is the convex hull of p and the joint numerical range $W(B_1, \dots, B_k)$ of k hermitian $s \times s$ matrices B_1, \dots, B_k for some $s < n$. If $\{p\}$ is a rank- r face, then $s = n - r$ is a valid choice.*

Proof. By Proposition 2.5, we have $A_1, \dots, A_k \in \mathbb{C}P \oplus P'M_nP'$, where $P \neq 0$ is the projection associated with $\{p\}$. This implies $A_iP = p_iP$, $i = 1, \dots, k$, where $p = (p_1, \dots, p_k)^\top \in \mathbb{R}^k$. Lemma 2.6 then shows that W is the convex hull of p and $W_{P'M_nP'}(P'A_1P', \dots, P'A_kP')$. Remark 2.3 (a) and (b) complete the proof. \square

An application of Lemma 2.6 or Corollary 2.7 requires describing the faces of the convex hull of two convex sets.

Lemma 2.8. *Let F be a face of the convex hull of two convex subsets Y_1, Y_2 of a real vector space. Then $F \cap Y_i$ is a face of Y_i , $i = 1, 2$, and $F = \text{conv}((F \cap Y_1) \cup (F \cap Y_2))$.*

Proof. Let $X := \text{conv}(Y_1 \cup Y_2)$. It is clear that $F \cap Y_i$ is a face of Y_i because F is a face of X and Y_i is a convex subset of X , $i = 1, 2$. The inclusion $F \supset \text{conv}((F \cap Y_1) \cup (F \cap Y_2))$ is clear since F is convex. Conversely, let $x \in F$. Then there exist $y_1 \in Y_1$, $y_2 \in Y_2$, and $s \in [0, 1]$ such that $x = (1 - s)y_1 + sy_2$. If $x = y_i$ for an $i = 1, 2$, then $x \in F \cap Y_i$ holds. Otherwise $s \in (0, 1)$ and $y_1, y_2 \in F$ follows because F is a face of X . \square

We recall the well-known relationship between Bonsall and Duncan's and the standard definition of the joint numerical range (1.1) and (1.2), respectively, in the setup of this section. Note that $\langle \varphi | A \varphi \rangle = \text{tr}(|\varphi\rangle\langle \varphi| A) = \langle |\varphi\rangle\langle \varphi|, A \rangle$ holds for every $A \in M_n$ and $|\varphi\rangle \in \mathbb{C}^n$. We denote the set of extreme points of a convex set C by $\text{ext } C$. Let $\text{range}(A) := \{A|\varphi\rangle : |\varphi\rangle \in \mathbb{C}^n\}$ denote the *range* of $A \in M_n$.

Lemma 2.9. *Let $P \in \mathcal{P}_n$ be a nonzero projection and let $F := w(\mathcal{D}_{PM_nP})$. Then*

$$F = \text{conv}[w(\text{ext } \mathcal{D}_{PM_nP})].$$

If $\dim(F) \leq 2$ or if $\dim(F) = 3$ and $\text{rk}(P) \geq 3$, then $F = w(\text{ext } \mathcal{D}_{PM_nP})$.

Proof. As a preliminary step, we recall that

$$\text{ext } \mathcal{D}_{PM_nP} = \{|\varphi\rangle\langle \varphi| : |\varphi\rangle \in \text{range}(P), \langle \varphi | \varphi \rangle = 1\}.$$

The extreme points of \mathcal{D}_n are parametrized by the map

$$\{|\varphi\rangle \in \mathbb{C}^n \mid \langle \varphi | \varphi \rangle = 1\} \rightarrow \text{ext } \mathcal{D}_n, \quad |\varphi\rangle \mapsto |\varphi\rangle\langle \varphi|,$$

see, e.g., [7, Section 5.1]. Clearly, a hermitian matrix $A \in \mathcal{H}_n$ is contained in PM_nP if and only if $\text{range}(A) \subset \text{range}(P)$. Since \mathcal{D}_{PM_nP} is a face of \mathcal{D}_n , a point in \mathcal{D}_{PM_nP} is an extreme point of \mathcal{D}_{PM_nP} if and only if it is an extreme point of \mathcal{D}_n .

Regarding the first assertion, observe that $w(\mathcal{D}_{PM_nP})$ is a linear image of the compact convex set \mathcal{D}_{PM_nP} . The claim is true because preimages of faces of F under $w|_{\mathcal{D}_{PM_nP}}$ are faces of \mathcal{D}_{PM_nP} and because every compact convex set is the convex hull of its extreme points (a statement known as the Minkowski-Steinitz theorem [55]).

Let $d = \dim(F)$ and $r = \text{rk}(P)$. There are a rotation $T : \mathbb{R}^k \rightarrow \mathbb{R}^k$, hermitian $B_1, \dots, B_d \in \mathcal{H}_r$, and $c \in \mathbb{R}^{k-d}$ such that $F = T^{-1}[W(B_1, \dots, B_d) \times \{c\}]$, as described in equation (2.12). Similarly, $w(\text{ext } \mathcal{D}_{PM_nP}) = T^{-1}[\tilde{W}(B_1, \dots, B_d) \times \{c\}]$. It is well known [5, 42] that $\tilde{W}(B_1, \dots, B_d)$ is convex in case $d \leq 2$ and in case $d = 3$ and $r \geq 3$. This proves the second assertion. \square

The assertion $W = \text{conv } \tilde{W}$ connecting the two definitions (1.1) and (1.2) of the joint numerical range is included in Lemma 2.9 for $P = \mathbf{1}_n$.

3. Numbers of non-elliptic faces

We describe all possible numbers that occur for the different types of non-elliptic faces of the joint numerical range $W := W(A_1, A_2, A_3)$ of three hermitian 4×4 matrices A_1, A_2, A_3 . We assume $\dim(W) = 3$.

Observe that every non-elliptic face of W is a rank-3 face because rank-2 faces are linear images of a three-dimensional Euclidean ball.

Lemma 3.1. *If a rank-3 face of W differs from a non-elliptic face of W , then both faces have dimension two. Their intersection is a one-dimensional face of each of them and an exposed face of W .*

Proof. Let F denote a non-elliptic face and G a rank-3 face. There exist orthogonal projections $P, Q \in \mathcal{P}_4$ such that $\mathcal{D}_{PM_4P} = w|_{\mathcal{D}_4}^{-1}(F)$ and $\mathcal{D}_{QM_4Q} = w|_{\mathcal{D}_4}^{-1}(G)$ by Theorem 2.1. Since P and Q have rank three, the intersection of their ranges is a two-dimensional subspace of \mathbb{C}^4 . Let $R \in \mathcal{P}_4$ denote the orthogonal projection onto this subspace. Then the preimage of $S := F \cap G$ is the three-dimensional ball $\mathcal{D}_{RM_4R} = w|_{\mathcal{D}_4}^{-1}(S)$. Therefore, S cannot be a singleton, as this would lead to the contradiction that F is an ellipse by [59, Lemma 4.5]. This shows that S is a segment. As F and G are exposed faces of W , so is $S = F \cap G$. \square

More details on the use of [59, Lemma 4.5] are explained in the following remark.

Remark 3.2 (The ellipticity criterion for bordered matrices). Let $R \leq P$ be the projections from the proof of Lemma 3.1, where $\text{rk}(P) = 3$ and $\text{rk}(R) = 2$. Then the joint numerical range $F = w_{A_1, A_2, A_3}(\mathcal{D}_{PM_4P})$ is affinely isomorphic to $W(B_1, B_2)$ for some hermitian 3×3 matrices B_1, B_2 by Remark 2.3 (d). We can choose B_1, B_2 such that the linear span of $\mathbf{1}_3, B_1, B_2$ is that of $\mathbf{1}_3, (UA_1U^*)[3], (UA_2U^*)[3], (UA_3U^*)[3]$, where $U \in M_4$ is a unitary that diagonalizes P to $UPU^* = \mathbf{1}_3 \oplus 0$. Let $R' \in \mathcal{P}_3$ be such that $URU^* = R' \oplus 0$. If the image of the three-dimensional ball \mathcal{D}_{RM_4R} under $w_{A_1, A_2, A_3} : \mathcal{H}_4 \rightarrow \mathbb{R}^3$ is an exposed point of F , then the image of $\mathcal{D}_{R'M_3R'}$ under $w_{B_1, B_2} : \mathcal{H}_3 \rightarrow \mathbb{R}^2$ is an exposed point of $W(B_1, B_2)$. Hence, [59, Lemma 4.5] proves that up to a unitary similarity of B_1 and B_2 and an affinity acting on $W(B_1, B_2)$ as in Remark 2.3 (c), one has

$$B_1 = \text{diag}(1, 0, 0) \quad \text{and} \quad B_2 = \begin{bmatrix} 0 & 0 & 1 \\ 0 & 0 & 0 \\ 1 & 0 & 0 \end{bmatrix}.$$

These are examples of *bordered matrices*: Every matrix entry that lies outside the first column and row vanishes. By [1, Proposition 3.2] the joint numerical range of any k linearly independent bordered hermitian $n \times n$ matrices is a k -dimensional ellipsoid in \mathbb{R}^k . Another test that corroborates that $W(B_1, B_2)$ is an ellipse is described in [11, Section 4].

Lemma 3.1 restricts the possible shapes of rank-3 faces of W significantly. Rank-3 faces that are ellipses, segments, or singletons can only exist if W has no non-elliptic faces. Otherwise, if W has a non-elliptic face, then any other rank-3 face is also a non-elliptic face.

Lemma 3.1 is no longer true if we modify its statement by replacing ‘non-elliptic’ with ‘rank-3’, as it is witnessed by the following example.

Example 3.3. The joint numerical range of the hermitian 3×3 matrices $\widehat{A}_1, \widehat{A}_2, \widehat{A}_3$ from [59, Example 6.3] has two ellipses on its boundary that intersect at the point $(-1, 0, 0)^\top$. We have $W(A_1, A_2, A_3) = W(\widehat{A}_1, \widehat{A}_2, \widehat{A}_3)$ if we extend $\widehat{A}_1, \widehat{A}_2, \widehat{A}_3$ to the hermitian 4×4 block diagonal matrices $A_1 := \widehat{A}_1 \oplus (-1)$, $A_2 := \widehat{A}_2 \oplus 0$, $A_3 := \widehat{A}_3 \oplus 0$. Then the two ellipses are rank-3 faces of $W(A_1, A_2, A_3)$ and they intersect at a single point.

Theorem 3.6 follows essentially from Lemma 3.1. Just one case needs to be excluded in Lemma 3.5. This is prepared by the following lemma, which is also used in the proof of Lemma 5.9.

Lemma 3.4. *The intersection of any three mutually distinct non-elliptic faces of W is a singleton which is a corner point of W . In particular, the three faces have a point in common.*

Proof. Let F_1, F_2, F_3 be three mutually distinct non-elliptic faces of W . Lemma 3.1 shows that $S_2 := F_1 \cap F_2$ and $S_3 := F_1 \cap F_3$ are one-dimensional exposed faces of W .

The intersection $F_1 \cap F_2 \cap F_3$ is empty or a singleton. Indeed, if S_2 were a face of F_3 , then by Proposition 2.4 the normal cone of S_2 would have three mutually distinct faces $N_W(F_i)$, $i = 1, 2, 3$ that are strictly included in $N_W(S_2)$ and differ from $\{0\}$. This would imply $\dim N_W(S_2) = 3$, contradicting the fact that S_2 is a segment. Therefore $F_1 \cap F_2 \cap F_3 = S_2 \cap F_3$ is a face of S_2 that is strictly included in S_2 : a singleton or the empty set.

Now we show that $F_1 \cap F_2 \cap F_3 \neq \emptyset$. By what is shown in the preceding paragraph, the segments S_2 and S_3 are different. Hence, the non-elliptic face F_1 , of which S_2 and S_3 are faces, is either a droplet or a triangle. In either case, S_2 and S_3 have a point in common.

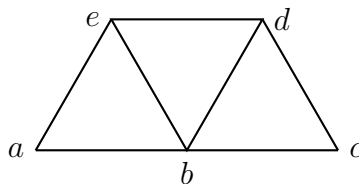
Let p be the unique point in $F_1 \cap F_2 \cap F_3$. The chain of exposed faces $F_1 \supset S_2 \supset \{p\}$ and Proposition 2.4 provide the strict inclusions of normal cones

$$N_W(F_1) \subset N_W(S_2) \subset N_W(p).$$

Since the ray $N_W(F_1)$ is a face of $N_W(S_2)$, which is a face of $N_W(p)$, it follows that the dimension of $N_W(p)$ is three. \square

Lemma 3.5. *If W has three mutually distinct triangular faces, then W is a tetrahedron.*

Proof. Lemma 3.1 and Lemma 3.4 show that the pairwise intersections of the triangles are three mutually distinct segments. The following figure depicts the triangles when one of them, the triangle bde , is glued to the other ones along shared sides.



For the three common edges of the triangles intersect at a point, it is evident that the faces abe and bcd intersect along $[b, a] = [b, c]$ and $a = c$.

The point b is a corner point of W by Lemma 3.4. Hence, Corollary 2.7 shows that W is the convex hull $W = \text{conv}(\{b\} \cup W')$ of b and the joint numerical range

W' of three hermitian 3×3 matrices. The triangle abe is a face of W and equals the convex hull

$$abe = \text{conv}(\{b\} \cup F)$$

of the corner point b and a face F of W' by Lemma 2.8. The inclusion $W' \subset abe$ is wrong because it implies $W = abe$ is a triangle. Hence, F is strictly included in W' , which means that F is a rank-1 or rank-2 face of W' , that is to say, a singleton, a segment, or a filled ellipse. Of these three choices, only the segment $F = [a, e]$ can fulfill $abe = \text{conv}(\{b\} \cup F)$.

Similarly, all three segments $[a, e]$, $[e, d]$, and $[d, c] = [d, a]$ are faces of W' . There is only one joint numerical range W' of three hermitian 3×3 matrices with three or more one-dimensional faces, see the introduction of [59]: the triangle. Hence, W is a tetrahedron. \square

Having the above lemmas, we are ready to prove the main classification result of the paper.

Theorem 3.6. *The numbers of non-elliptic faces of the joint numerical range W belong to one of the following 15 columns.*

<i>type</i>	<i>shape</i>	<i>count</i>														
0	<i>oval</i>	0	1	0	0	0	0	0	0	0	0	0	0	0	0	
1	<i>loaf</i>	0	0	1	2	1	1	0	0	0	0	0	0	0	0	
2	<i>droplet</i>	0	0	0	0	1	0	1	2	3	1	1	2	0	0	
3	<i>triangle</i>	0	0	0	0	0	1	0	0	0	1	2	1	1	2	
<i>example no.</i>		0	1	2	3	4	5	6	7	8	9	10	11	12	13	14

All 15 tuples are attained by respective examples presented in Section 4 below. Every tuple described by the columns 8–11 or 13–14 implies the existence of a corner point of W .

Proof. The table can be derived from the fact that any two distinct non-elliptic faces intersect along a segment (Lemma 3.1).

Let $a_i \in \mathbb{Z}_{\geq 0}$ denote the number of non-elliptic faces of type i of W , $i = 0, 1, 2, 3$. A face of type 0 cannot intersect any other non-elliptic face, hence $a_0 > 0$ implies $a_1 = a_2 = a_3 = 0$ and $a_0 = 1$. Similarly, if $a_0 = 0$ and $a_1 \geq 1$, then $a_1 + a_2 + a_3 \leq 2$. Also, if $a_0 = a_1 = 0$ and $a_2 \geq 1$, then $a_2 + a_3 \leq 3$. Finally, $a_3 \leq 4$. The numbers $a_0 = a_1 = a_2 = 0$ and $a_3 = 3$ are excluded by Lemma 3.5.

The existence of a corner point follows from Lemma 3.4 for the columns 8, 10, 11, and 14, and from Theorem 5.10 for the columns 9 and 13. \square

4. Examples

Here we present examples of hermitian 4×4 matrices A_1, A_2, A_3 with joint numerical ranges $W = W(A_1, A_2, A_3)$ having all possible numbers of non-elliptic faces

listed in Theorem 3.6. Figure 4.1 shows W of all the examples with non-elliptic faces highlighted. Proving that each rank-3 face has the specified non-elliptic shape and that W has no further rank-3 faces is a straightforward application of the methods of Remark 4.2 and Remark 4.3, and is therefore omitted.

Definition 4.1. Let $u_0, u_1, u_2, u_3 \in \mathbb{R}$, $A := u_0\mathbb{1}_4 + u_1A_1 + u_2A_2 + u_3A_3$, and let $A\{i, j\}$ ($i \neq j$) be the principal minor of A that is the determinant of the submatrix obtained by deleting all the rows and columns except for those with the indices $i, j \in \{1, 2, 3, 4\}$. Similarly, $A\{i, j, k\}$ is a principal minor of order three. If A has rank one, then we call (u_0, u_1, u_2, u_3) a *rank-1 tuple* and we refer to the kernel projection of A as the *kernel projection* of (u_0, u_1, u_2, u_3) .

Remark 4.2 (Controlling rank-3 and non-elliptic faces). A necessary condition for the existence of a non-elliptic face is that a rank-1 tuple (u_0, u_1, u_2, u_3) exists. More specifically, every non-elliptic face F of W is a rank-3 face of W . It has the form $F = w(\mathcal{D}_{PM_4P})$, where $P \in \mathcal{P}_n$ is the rank-3 projection associated to F . Since F is an exposed face of W , there are $u_1, u_2, u_3 \in \mathbb{R}$ such that P is the spectral projection of $u_1A_1 + u_2A_2 + u_3A_3$ with respect to the smallest eigenvalue by Theorem 2.1. Equivalently, there is a rank-1 tuple (u_0, u_1, u_2, u_3) whose kernel projection is P . The rank-one condition is rather easy to verify in terms of vanishing of the six order two principal minors

$$A\{1, 2\}, \quad A\{1, 3\}, \quad A\{1, 4\}, \quad A\{2, 3\}, \quad A\{2, 4\}, \quad A\{3, 4\}$$

and the four order three principal minors

$$A\{1, 2, 3\}, \quad A\{1, 2, 4\}, \quad A\{1, 3, 4\}, \quad A\{2, 3, 4\}$$

of $A = u_0\mathbb{1}_4 + u_1A_1 + u_2A_2 + u_3A_3$, see [15], Theorem 16 of Chapter IV.

Remark 4.3 (Deciding on the shape of a rank-3 face). Let $P \in \mathcal{P}_n$ be a rank-3 projection and let $F := w(\mathcal{D}_{PM_4P})$. For example, if (u_0, u_1, u_2, u_3) is a rank-1 tuple, whose kernel projection is P , then F is a rank-3 face of W .

(a) **Employing 3×3 matrices.** Let B_1, B_2 be hermitian 3×3 matrices such that the linear span of the matrices $\mathbb{1}_3, B_1, B_2$ is the same as that of

$$\mathbb{1}_3, \quad (UA_1U^*)[3], \quad (UA_2U^*)[3], \quad (UA_3U^*)[3],$$

where $U \in M_4$ is a unitary such that $UPU^* = \mathbb{1}_3 \oplus 0$. Then Remark 2.3 (d) guarantees that F is affinely isomorphic to the joint numerical range $W(B_1, B_2)$.

(b) **Invoking the numerical range.** One can also use the numerical range $\tilde{W}(B)$ of

$$B := B_1 + iB_2$$

to decide on the shape of $F \cong W(B_1, B_1)$ because $W(B_1, B_1) = \tilde{W}(B)$ holds as recalled in (1.3). We employ Kippenhahn's classification to decide on the shape of $\tilde{W}(B)$.

- (c) **Deciding unitary reducibility.** A square matrix is *unitarily reducible* if it is unitarily similar to a block diagonal matrix with at least two proper blocks. Otherwise the matrix is *unitarily irreducible*. We claim that the 3×3 matrix B is unitarily irreducible if and only if the positive semidefinite matrix

$$S := [B_1, B_2]^*[B_1, B_2] + [B_1^2, B_2]^*[B_1^2, B_2] + [B_1, B_2^2]^*[B_1, B_2^2] + [B_1^2, B_2^2]^*[B_1^2, B_2^2]$$

is positive definite, where $[X, Y] := XY - YX$ is the commutator of $X, Y \in \mathcal{H}_3$. The Sylvester criterion allows us to decide the positive definiteness of S easily.

We prove our claim. If B is unitarily reducible then it generates a unital $*$ -algebra (the smallest $*$ -algebra on \mathbb{C}^3 containing B and $\mathbf{1}_3$) that is strictly smaller than M_3 . The converse is also true since any unital $*$ -algebra on \mathbb{C}^3 has a block diagonal form up to unitary similarity (see, e.g., [17, Theorem 5.6]). Clearly, the unital $*$ -algebra generated by B is the set of the values of all noncommutative polynomials in the variables B_1 and B_2 (we identify scalars with scalar matrices). According to [4], Theorem 8, B generates the unital $*$ -algebra M_3 if and only if S is positive definite.

- (d) **The unitarily reducible case.** Let B be unitarily reducible.

- If B_1 and B_2 commute, then B is normal and $\tilde{W}(B)$ is the convex hull of the three eigenvalues of B , which is a triangle if and only if the eigenvalues are real affinely independent.
- If B_1 and B_2 do not commute then the curve $p_B = 0$ in $\mathbb{C}\mathbb{P}^2$ defined by the polynomial (1.4) is the union of a conic e and a line ℓ . The Kippenhahn curve $C_{\mathbb{R}}(B)$ is the union of an ellipse e^* and a point p in \mathbb{R}^2 . By substituting the equation of ℓ into that of e , it is easy to compute the two points in $e \cap \ell$. They are distinct and real if and only if p lies outside e^* , if and only if $\tilde{W}(B)$ is a droplet.

- (e) **The unitarily irreducible case.** Let B be unitarily irreducible. Then $\tilde{W}(B)$ is an ellipse, a loaf, or an oval. We use conditions from [36] to distinguish these shapes.

- **Ellipses.** Let $\lambda_1, \lambda_2, \lambda_3$ be the eigenvalues of B . By [36, Theorem 2.3], the Kippenhahn curve $C_{\mathbb{R}}(B)$ consists of an ellipse and a point if and only if
 - the number $\delta := \operatorname{tr}(B^*B) - \sum_{i=1}^3 |\lambda_i|^2$ is strictly positive and
 - the number $\lambda := \operatorname{tr}(B) + \frac{1}{\delta}(\sum_{i=1}^3 |\lambda_i|^2 \lambda_i - \operatorname{tr}(B^*B^2))$ coincides with at least one of the eigenvalues of B .

If these conditions are satisfied⁶, then $C_{\mathbb{R}}(B)$ is the union of λ and the ellipse having its foci at two other eigenvalues of B and minor axis of length $\sqrt{\delta}$.

⁶We remark that λ lies strictly inside the ellipse (not on the boundary of $\tilde{W}(B)$) by [32, Theorem 1.6.6] because B is unitarily irreducible.

Ellipticity criteria in some other settings can be found in [1, Proposition 3.2] and in [11, Section 4], see Remark 3.2 above.

- **Loafs.** By [36, Proposition 3.2], the numerical range $\tilde{W}(B)$ is a loaf if and only if there are real $u_0, u_1, u_2 \in \mathbb{R}$ such that $u_0\mathbb{1}_3 + u_1B_1 + u_2B_2$ has rank one. This matrix has rank one if and only if its three principal minors of order two and its determinant are zero (see [15, p. 79]).
- **Ovals.** The preceding conditions for $\tilde{W}(B)$ to be an ellipse or a loaf are not just sufficient but also necessary. Hence, their failure proves that $\tilde{W}(B)$ is an oval.

The remainder of this section presents examples. They are all depicted in Figure 4.1.

Example E0. No faces: $a_0 = a_1 = a_2 = a_3 = 0$

This is the generic case (see [25, Proposition 4.9] and [59, Theorem 4.2]). Exemplary matrices:

$$\begin{bmatrix} 0 & 1 & 0 & 0 \\ 1 & 0 & i & 0 \\ 0 & -i & 0 & 0 \\ 0 & 0 & 0 & 0 \end{bmatrix}, \begin{bmatrix} 0 & 0 & 0 & 0 \\ 0 & 0 & 1 & 0 \\ 0 & 1 & 0 & i \\ 0 & 0 & -i & 0 \end{bmatrix}, \begin{bmatrix} 0 & 0 & 0 & i \\ 0 & 0 & 0 & 0 \\ 0 & 0 & 0 & 1 \\ -i & 0 & 1 & 0 \end{bmatrix}$$

There are no rank-1 tuples.

Example E1. Single oval face: $a_0 = 1$ and $a_1 = a_2 = a_3 = 0$

Exemplary matrices:

$$\begin{bmatrix} 0 & i & i & -2 \\ -i & 0 & i & 2 \\ -i & -i & 0 & 2i \\ -2 & 2 & -2i & 0 \end{bmatrix}, \begin{bmatrix} -2 & 1 & 1 & -2i \\ 1 & 1 & 1 & 2i \\ 1 & 1 & 1 & 2 \\ 2i & -2i & 2 & 0 \end{bmatrix}, \text{diag}(0, 0, 0, -4)$$

Rank-1 tuple: $(0, 0, 0, 1)$

Note that examples with one particular face can be constructed by extending a 3×3 matrix (pair of hermitian matrices) with appropriate numerical range. See also Examples E2, E6 and E12.

Example E2. Single loaf face: $a_1 = 1, a_0 = a_2 = a_3 = 0$

Exemplary matrices:

$$\begin{bmatrix} 0 & 0 & 0 & 1 \\ 0 & 0 & 0 & -1 \\ 0 & 0 & -\sqrt{2} & -i \\ 1 & -1 & i & 0 \end{bmatrix}, \begin{bmatrix} -\frac{1}{\sqrt{2}} & 0 & \frac{i}{\sqrt{2}} & -i \\ 0 & \frac{1}{\sqrt{2}} & \frac{i}{\sqrt{2}} & i \\ -\frac{i}{\sqrt{2}} & -\frac{i}{\sqrt{2}} & 0 & 1 \\ i & -i & 1 & 0 \end{bmatrix}, \text{diag}(0, 0, 0, 2)$$

Rank-1 tuple: $(0, 0, 0, 1)$

This example is constructed in an analogous way as Example E1.

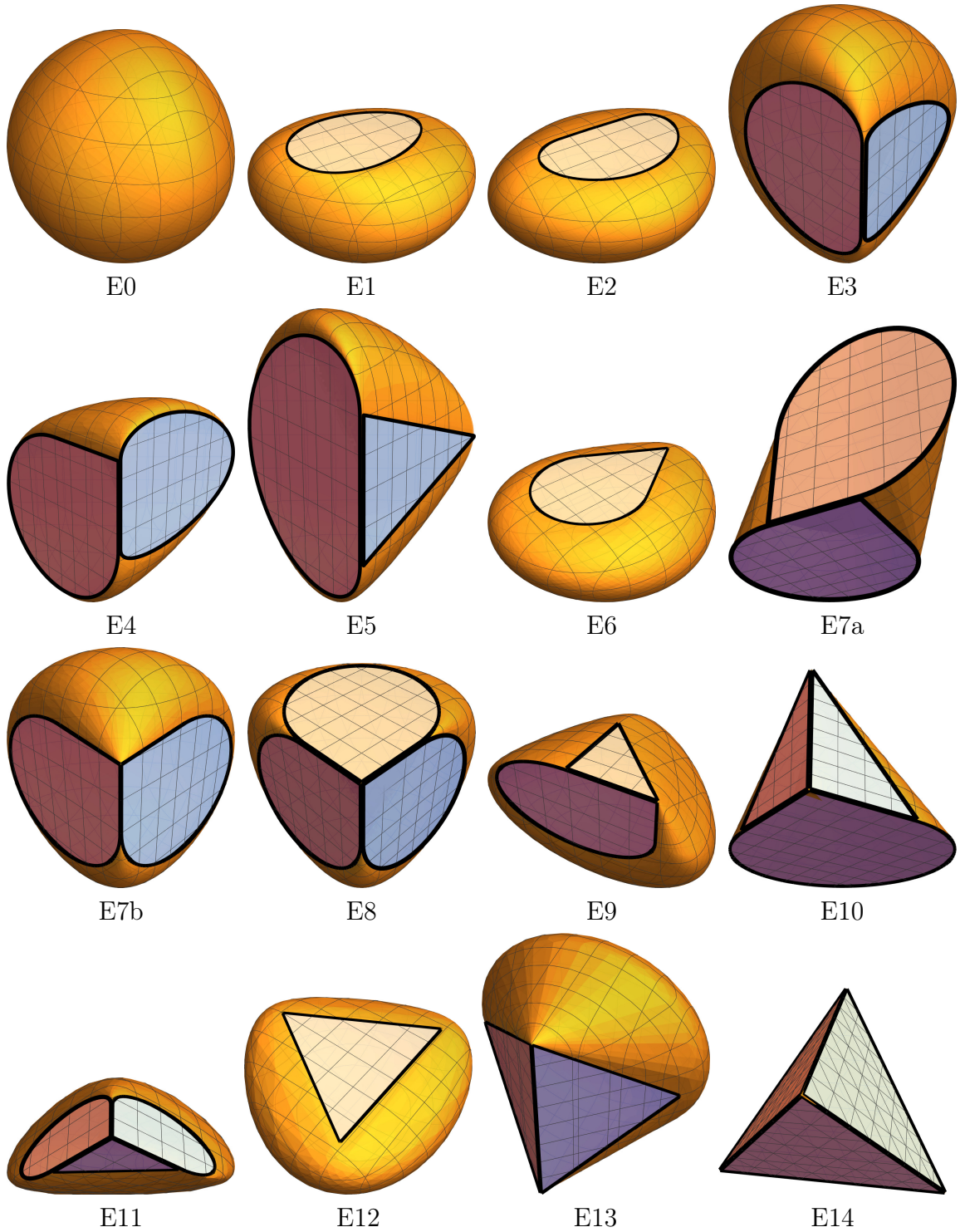


Figure 4.1: Exempls belonging to 15 classes of joint numerical ranges of 3 hermitian matrices of order 4 concerning the non-elliptic faces listed in Theorem 3.6 and analyzed in Section 4.

Example E3. Two loaf faces: $a_1 = 2$ and $a_0 = a_2 = a_3 = 0$
Exemplary matrices are

$$\text{diag}(1, 1, 1, 0), F \text{diag}(1, 1, 1, 0)F^*, \frac{1}{2} \begin{bmatrix} 0 & 1 & 0 & -1 \\ 1 & 0 & 0 & 0 \\ 0 & 0 & 0 & 0 \\ -1 & 0 & 0 & 0 \end{bmatrix},$$

where $F = (F_{i,j})_{i,j=1}^4 = \frac{1}{2}(i^{(i-1)}(j-1))_{i,j=1}^4$ is the unitary Fourier matrix of order 4.
Rank-1 tuples: $(-1, 1, 0, 0)$ and $(-1, 0, 1, 0)$

Example E4. A loaf and a droplet face: $a_1 = a_2 = 1$ and $a_0 = a_3 = 0$
Exemplary matrices:

$$\text{diag}(2, 0, 0, 0), \begin{bmatrix} 0 & 0 & 0 & 0 \\ 0 & 0 & 0 & 0 \\ 0 & 0 & 1 & i \\ 0 & 0 & -i & 1 \end{bmatrix}, \begin{bmatrix} \frac{1}{2} & -\frac{1}{2} & \frac{1}{2} & 0 \\ -\frac{1}{2} & 1 & 0 & 0 \\ \frac{1}{2} & 0 & 0 & 1 \\ 0 & 0 & 1 & 0 \end{bmatrix}$$

Rank-1 tuples: $(0, 1, 0, 0)$ and $(0, 0, 1, 0)$

Example E5. A loaf and a triangular face: $a_1 = a_3 = 1$ and $a_0 = a_2 = 0$
Exemplary matrices:

$$\text{diag}(0, 0, 0, 1), \text{diag}(0, 0, 1, 0), \frac{1}{2} \begin{bmatrix} -1 & 0 & -i & 0 \\ 0 & 1 & 1 & 0 \\ i & 1 & 0 & 1 \\ 0 & 0 & 1 & 0 \end{bmatrix}$$

Rank-1 tuples: $(0, 1, 0, 0)$ and $(0, 0, 1, 0)$

Example E6. Single droplet face: $a_2 = 1$ and $a_0 = a_1 = a_3 = 0$
Exemplary matrices:

$$\begin{bmatrix} -1 & 1 & 0 & -1 \\ 1 & -1 & 0 & 1 \\ 0 & 0 & 1 & i \\ -1 & 1 & -i & 0 \end{bmatrix}, \begin{bmatrix} 0 & -i & 0 & -i \\ i & 0 & 0 & i \\ 0 & 0 & 0 & 1 \\ i & -i & 1 & 0 \end{bmatrix}, \text{diag}(0, 0, 0, -2)$$

Rank-1 tuple: $(0, 0, 0, 1)$

The appropriate triple of hermitian matrices can be constructed in the same way as in the case of other unique rank-3 faces (cf. Examples E1 and E2). A different construction is described in Remark 5.7 (b).

Example E7a. *Yin-Yang configuration of droplet faces:* $a_0 = a_1 = a_3 = 0$ and $a_2 = 2$

Exemplary matrices:

$$\begin{bmatrix} 0 & 0 & 0 & 0 \\ 0 & 0 & 0 & 0 \\ 0 & 0 & 1 & 1 \\ 0 & 0 & 1 & 1 \end{bmatrix}, \begin{bmatrix} 0 & 1 & 0 & 0 \\ 1 & 0 & 0 & 0 \\ 0 & 0 & 1 & i \\ 0 & 0 & -i & 1 \end{bmatrix}, \begin{bmatrix} 1 & i & 0 & 0 \\ -i & 1 & 0 & 0 \\ 0 & 0 & 0 & 0 \\ 0 & 0 & 0 & 0 \end{bmatrix}$$

Rank-1 tuples: $(0, 1, 0, 0)$ and $(0, 0, 0, 1)$

The joint numerical range is the convex hull of two orthogonal circles with centers $(0, 0, 1)$ and $(1, 1, 0)$. The intersection of the two droplet faces is the segment with endpoints $(0, 0, 0)$ and $(0, 1, 0)$.

Example E7b. Another example of two droplets: $a_2 = 2$ and $a_0 = a_1 = a_3 = 0$

Exemplary matrices:

$$\begin{bmatrix} -1 & 0 & \sqrt{2} & 0 \\ 0 & 1 & 0 & 0 \\ \sqrt{2} & 0 & 0 & 0 \\ 0 & 0 & 0 & 1 \end{bmatrix}, \begin{bmatrix} -1 & 0 & -\sqrt{2} & 0 \\ 0 & 1 & 0 & 0 \\ -\sqrt{2} & 0 & 0 & 0 \\ 0 & 0 & 0 & 1 \end{bmatrix}, \begin{bmatrix} 0 & 2 & 0 & 0 \\ 2 & 0 & 0 & 0 \\ 0 & 0 & 0 & 0 \\ 0 & 0 & 0 & 1 \end{bmatrix}$$

Rank-1 tuples: $(-1, 1, 0, 0)$ and $(-1, 0, 1, 0)$

This example was constructed by adding a corner point to a joint numerical range of matrices of order 3 having two elliptic faces (an affine transformation of [59, Example 6.3]).

Example E8. Three droplet faces: $a_2 = 3$ and $a_0 = a_1 = a_3 = 0$

Exemplary matrices:

$$\begin{bmatrix} 2 & 0 & 0 & 0 \\ 0 & 2 & 0 & 0 \\ 0 & 0 & 1 & i \\ 0 & 0 & -i & 1 \end{bmatrix}, \begin{bmatrix} 1 & 0 & -i & 0 \\ 0 & 2 & 0 & 0 \\ i & 0 & 1 & 0 \\ 0 & 0 & 0 & 2 \end{bmatrix}, \begin{bmatrix} 1 & 0 & 0 & i \\ 0 & 2 & 0 & 0 \\ 0 & 0 & 2 & 0 \\ -i & 0 & 0 & 1 \end{bmatrix}$$

Rank-1 tuples: $(-2, 1, 0, 0)$, $(-2, 0, 1, 0)$, and $(-2, 0, 0, 1)$

Example E9. A droplet and a triangular face: $a_2 = a_3 = 1$ and $a_0 = a_1 = 0$

Exemplary matrices:

$$\begin{bmatrix} 1 & 0 & 0 & 0 \\ 0 & 0 & 1 & 0 \\ 0 & 1 & 0 & 0 \\ 0 & 0 & 0 & 1 \end{bmatrix}, \begin{bmatrix} 0 & 0 & \sqrt{2} & 0 \\ 0 & 0 & 0 & 0 \\ \sqrt{2} & 0 & 0 & 0 \\ 0 & 0 & 0 & 1 \end{bmatrix}, \text{diag}(0, 0, -2, 0)$$

Rank-1 tuples: $(0, 0, 0, 1)$ and $(-1, 1, 0, 0)$

This example was obtained by adding a corner point to the joint numerical range of three hermitian 3×3 matrices having one ellipse and one segment on its boundary (cf. [59, Example 6.7]). The corner point in this class is inevitable, see Theorem 5.10.

Example E10. A droplet and two triangular faces: $a_2 = 1, a_3 = 2$ and $a_0 = a_1 = 0$
Exemplary matrices:

$$\begin{bmatrix} 1 & -i & 0 & 0 \\ i & 1 & 0 & 0 \\ 0 & 0 & 0 & 0 \\ 0 & 0 & 0 & 0 \end{bmatrix}, \begin{bmatrix} 0 & 1 & 0 & 0 \\ 1 & 0 & 0 & 0 \\ 0 & 0 & 1 & 0 \\ 0 & 0 & 0 & 1 \end{bmatrix}, \text{diag}(0, 0, 1, 0)$$

Rank-1 tuples: $(0, 0, 0, 1)$, $(-1, 0, 1, 0)$, and $(0, 1, 0, 0)$

The triple of matrices is unitarily reducible and hence the joint numerical range is the convex hull of the points $(0, 1, 1)$, $(0, 1, 0)$, and the circle in the x - y -plane with center $(1, 0, 0)$ and radius 1. The configuration of faces can be recovered using Lemma 2.8.

Note that due to Theorem 5.10, the example of this class necessarily has two corner points (endpoints of the common edge of the triangular faces), hence it is a convex hull of a segment and an ellipsoid (the joint numerical range of 2×2 matrices). Unless the latter is degenerated to an ellipse coplanar with exactly one of the corners, the droplet face cannot appear (cf. Lemma 2.8).

Example E11. Two droplets and a triangle: $a_2 = 2, a_3 = 1$, and $a_0 = a_1 = 0$
Exemplary matrices:

$$\begin{bmatrix} 1 & 0 & i\sqrt{2} & 0 \\ 0 & 0 & 0 & 0 \\ -i\sqrt{2} & 0 & 2 & 0 \\ 0 & 0 & 0 & 0 \end{bmatrix}, \begin{bmatrix} 0 & 0 & 0 & 0 \\ 0 & 1 & -i\sqrt{2} & 0 \\ 0 & i\sqrt{2} & 2 & 0 \\ 0 & 0 & 0 & 0 \end{bmatrix}, \text{diag}(0, 0, 2, 0)$$

Rank-1 tuples: $(0, 1, 0, 0)$, $(0, 0, 1, 0)$, and $(0, 0, 0, 1)$

An example of this type can be obtained by adding a corner point to the joint numerical range of 3×3 matrices having two ellipses and a segment in the boundary (see [59, Example 6.3]). According to Lemma 3.4, there has to be a corner point and all examples in the class share this construction (cf. also Lemma 2.8).

Example E12. Single triangular face: $a_3 = 1$ and $a_0 = a_1 = a_2 = 0$
Exemplary matrices:

$$\begin{bmatrix} \sqrt{3} & 0 & 0 & -1 \\ 0 & -\frac{\sqrt{3}}{2} & 0 & 1 \\ 0 & 0 & -\frac{\sqrt{3}}{2} & -i \\ -1 & 1 & i & 0 \end{bmatrix}, \begin{bmatrix} 0 & 0 & 0 & i \\ 0 & \frac{3}{2} & 0 & -i \\ 0 & 0 & -\frac{3}{2} & 1 \\ -i & i & 1 & 0 \end{bmatrix}, \text{diag}(0, 0, 0, -2)$$

Rank-1 tuple: $(0, 0, 0, 1)$

This example is constructed similarly to Examples E1, E2 and E6.

Example E13. Two triangular faces: $a_3 = 2$ and $a_0 = a_1 = a_2 = 0$
 Exemplary matrices:

$$\text{diag}(0, 0, 1, -1), \begin{bmatrix} 1 & 0 & 0 & 0 \\ 0 & 1 & 0 & 0 \\ 0 & 0 & 0 & \frac{1}{2} \\ 0 & 0 & \frac{1}{2} & 0 \end{bmatrix}, \begin{bmatrix} 0 & 1 & 0 & 0 \\ 1 & 0 & 0 & 0 \\ 0 & 0 & 0 & -i \\ 0 & 0 & i & 0 \end{bmatrix}$$

Rank-1 tuples: $(-2, \sqrt{3}, 2, 0)$ and $(-2, -\sqrt{3}, 2, 0)$

By Theorem 5.10, the joint numerical range in this class has two corner points and therefore the matrices admit a common two-dimensional reducing subspace. The joint numerical range is necessarily the convex hull of two points and a, possibly degenerated, ellipsoid E , similarly as in Example E10. The ellipsoid E cannot intersect the segment between the corners and cannot be enclosed in a plane containing one of them (the latter would lead to class no. 10 or no. 14).

Example E14. Four triangular faces: $a_3 = 4$ and $a_0 = a_1 = a_2 = 0$
 Exemplary matrices:

$$\text{diag}(1, 1, -1, -1), \text{diag}(1, -1, 1, -1), \text{diag}(1, -1, -1, 1)$$

The case $a_3 = 4$ is attained solely in case of the joint numerical range being a tetrahedron. For every tetrahedral joint numerical range, there exists an orthonormal basis simultaneously diagonalizing all three matrices.

5. One-dimensional faces and corner points

Let A_1, A_2, A_3 be hermitian $n \times n$ matrices and let $W = W(A_1, A_2, A_3)$ have dimension $\dim(W) = 3$. We prove that the intersection of any three mutually distinct one-dimensional faces of W that have a point in common is a corner point of W if $n = 4$. A counterexample is given for $n = 5$.

Remark 5.1 (Recurrent arguments). (a) Every one-dimensional nonexposed face G_1 of W is an exposed face of a two-dimensional exposed face H_1 of W , see the discussion below equation (2.5). The face H_1 is unique (because a one-dimensional face that is included in two distinct two-dimensional exposed faces is exposed). If $n = 4$, then H_1 is an example of what we call a non-elliptic face in Definition 1.1.

(b) If two or more mutually distinct one-dimensional faces of W have a point in common, then their intersection is an extreme point of W (because the infimum in the lattice of faces is the intersection).

Lemma 5.2. *Let three mutually distinct one-dimensional faces of W , at least two of which are exposed, have a point in common. Then their intersection is a corner point of W .*

Proof. Let G_1, G_2, G_3 denote the one-dimensional faces in question and assume that G_2, G_3 are exposed. Then $G_2 \cap G_3 = \{p\}$ holds for an exposed point p of W , as the infimum in the lattice of exposed faces is the intersection. Also, $G_1 \cap G_2 \cap G_3 = \{p\}$.

If G_1 is exposed then, by Proposition 2.4, the normal cones $N_W(G_1), N_W(G_2), N_W(G_3)$ are rays or two-dimensional convex cones that are mutually distinct and that are proper faces of $N_W(p)$. This implies $\dim N_W(p) = 3$. Let G_1 be a nonexposed face and H_1 the unique two-dimensional face containing G_1 . The same argument as before when $N_W(G_1)$ is replaced with $N_W(H_1)$ proves $\dim N_W(p) = 3$. \square

Example 5.3 shows that the conclusion of Lemma 5.2 is no longer valid for 5×5 matrices under the weaker assumption that only one of the one-dimensional faces is exposed. Therefore, Theorem 5.10 is a special result on 4×4 matrices, not applicable to matrices of higher order.

Example 5.3. Consider the convex set C in \mathbb{R}^3 that is the convex hull of the unit circle in the y - z -plane and the triangle with vertices $p_1 := (-1, -1, 0)^\top$, $p_2 := (-1, 1, 0)^\top$, $p_3 := (1, 0, 0)^\top$ in the x - y -plane.

The segments $[p_1, q]$ and $[p_2, q]$ are nonexposed faces of C and the segment $[p_3, q]$ is an exposed face of C . All three segments lie in the boundary of C and intersect at the point $q := (0, 0, 1)^\top$. But, q is not a corner point of C . Note that C can be realized as the joint numerical range of the hermitian 5×5 matrices

$$\begin{bmatrix} 0 & 0 \\ 0 & 0 \end{bmatrix} \oplus \text{diag}(-1, -1, 1), \quad \begin{bmatrix} 0 & 1 \\ 1 & 0 \end{bmatrix} \oplus \text{diag}(-1, 1, 0), \quad \begin{bmatrix} 0 & -i \\ i & 0 \end{bmatrix} \oplus \text{diag}(0, 0, 0),$$

which (by Lemma 2.6 and Remark 2.3 (b)) is the convex hull of the unit disk

$$W \left(\begin{bmatrix} 0 & 0 \\ 0 & 0 \end{bmatrix}, \begin{bmatrix} 0 & 1 \\ 1 & 0 \end{bmatrix}, \begin{bmatrix} 0 & -i \\ i & 0 \end{bmatrix} \right)$$

in the y - z -plane and the points p_1, p_2, p_3 in the x - y -plane.

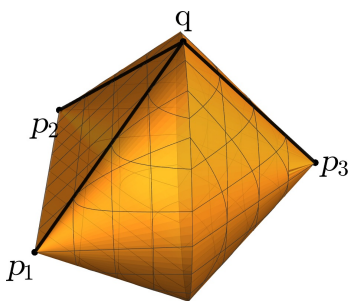


Figure 5.1: The joint numerical range C described in Example 5.3. The point q is not a corner point of C although it is the intersection of three mutually distinct one-dimensional faces of C . This can only happen for matrices of order five or greater by Theorem 5.10.

From here on, the hermitian matrices A_1, A_2, A_3 are assumed to have dimension $n = 4$. In the following Lemma 5.4, we simplify the matrices A_1, A_2, A_3 using the access sequence technique of Theorem 2.1 and we customize the notation.

Lemma 5.4. *Suppose that W has a non-elliptic face F_1 . Suppose further that F_1 has a one-dimensional face F_2 that intersects a one-dimensional exposed face G of W and $G \neq F_2$. Then $F_2 \cap G = \{p\}$ is a singleton, which is an extreme point of W . Up to a unitary similarity and an invertible affine transformation, the access sequence of faces $W \supset F_1 \supset F_2 \supset \{p\}$ corresponds to the access sequence $\mathbb{1}_4 \geq P_1 \geq P_2 \geq P_3$ of orthogonal projections*

$$P_1 = \text{diag}(1, 1, 1, 0), \quad P_2 = \text{diag}(1, 1, 0, 0), \quad P_3 = \text{diag}(1, 0, 0, 0),$$

and

$$A_1 = \text{diag}(0, 0, 0, 1), \quad A_2 = 0 \oplus C, \quad A_3 = \begin{bmatrix} \text{diag}(0, 0, 1) & |\varphi\rangle \\ \langle\varphi| & 0 \end{bmatrix}, \quad (5.1)$$

where $C \in M_3$ is positive semidefinite of rank two and $|\varphi\rangle = (w_1, w_2, w_3)^\top \in \mathbb{C}^3$. Note $p = (0, 0, 0)^\top$. The projection associated to G is the kernel projection of A_2 .

Proof. Since $F_2 \cap G = \{p\}$ is an extreme point of W , it follows that p is an endpoint of the segment F_2 (and of G). We can therefore use the access sequences provided in Example 2.2. The projection Q associated to G has rank $\text{rk}(Q) = 2$. Otherwise, $\text{rk}(Q) = 3$ would contradict Lemma 3.1 because $G \neq F_1$.

We analyze the exposed faces F_1 and G using access sequences of lengths one. Applying an invertible affinity as described by the equations (2.9) and (2.10), we can take A_1 (resp., A_2) such that P_1 (resp., Q) is the spectral projection of A_1 (resp., A_2) corresponding to the smallest eigenvalue. Thus, we take $A_1 = \text{diag}(0, 0, 0, 1)$ and A_2 a positive semidefinite matrix of rank two. Then $A_2 = 0 \oplus C$ holds for a positive semidefinite 3×3 matrix C , because $P_3 \leq Q$ is implied by $p \in G$. We write

$$C = \begin{bmatrix} B & |\eta\rangle \\ \langle\eta| & a \end{bmatrix}, \quad A_2 = 0 \oplus \begin{bmatrix} B & |\eta\rangle \\ \langle\eta| & a \end{bmatrix}, \quad \text{and} \quad A_3 = \begin{bmatrix} D & |\xi\rangle \\ \langle\xi| & 0 \end{bmatrix},$$

where $B \in M_2$ is positive semidefinite, $|\eta\rangle \in \mathbb{C}^2$, $a \geq 0$, $D \in M_3$ is hermitian, and $|\xi\rangle \in \mathbb{C}^3$. The bottom right entry of A_3 was tacitly erased adding a scalar multiple of A_1 to A_3 .

Considering the access sequence $\mathbb{1}_4 \geq P_1 \geq P_2$ of length two, we know that P_2 is the spectral projection of a linear combination of matrices $P_1 A_i P_1$, $i = 1, 2, 3$, corresponding to the smallest spectral value in the algebra $M_3 \oplus 0$. There exist $\lambda_1, \lambda_2, \lambda_3 \in \mathbb{R}$ such that

$$\begin{aligned} \text{diag}(0, 0, 1) \oplus 0 &= P_1(\lambda_1 \mathbb{1}_4 + \lambda_2 A_2 + \lambda_3 A_3) P_1 \\ &= (\lambda_1 \mathbb{1}_3 + \lambda_2(0 \oplus B) + \lambda_3 D) \oplus 0. \end{aligned} \quad (5.2)$$

A solution to equation (5.2) exists by Theorem 2.1. We use it to solve for D . First, note that $\lambda_1 = \lambda_3 = 0$ is not possible, because B is not a scalar multiple of $\text{diag}(0, 1)$. If it were, then $C \geq 0$ would imply $|\eta\rangle = (0, z)^\top$ for some $z \in \mathbb{C}$, see for example [33]. Then $P_2 = Q$ would be the kernel projection of A_2 in contradiction to the

assumption $F_2 \neq G$. Second, $\lambda_1 \neq \lambda_3 = 0$ is not possible, as the top left entries of the two sides of equation (5.2) would differ. This proves $\lambda_3 \neq 0$ and shows that there are $s_1, s_2, s_3 \in \mathbb{R}$ such that $s_3 \neq 0$ and

$$D = s_1 \mathbf{1}_3 + s_2(0 \oplus B) + s_3 \text{diag}(0, 0, 1).$$

Applying another affinity, we replace A_3 with $A_3 - s_1 \mathbf{1}_4 + (s_1 + as_2)A_1 - s_2 A_2$ divided by s_3 . This yields the matrices above. \square

The following lemma deserves to be stated explicitly as it is used twice, in Propositions 5.6 and 5.8.

Lemma 5.5. *Assume $A_1, A_2, A_3 \in \mathbb{C}P \oplus P'M_4P'$, where $P \in \mathcal{P}_4$ is a nonzero orthogonal projection and $P' := \mathbf{1}_4 - P$. Let $p_i \in \mathbb{R}$ be such that $A_i P = p_i P$, $i = 1, 2, 3$. If W has a one-dimensional nonexposed face, then $(p_1, p_2, p_3)^\top$ is a corner point of W .*

Proof. Let $s < 4$ be the rank of the projection $P' = \mathbf{1}_4 - P$. By Lemma 2.6, the joint numerical range W is the convex hull of p and the joint numerical range

$$W' := W_{P'M_n P'}(P'A_1 P', P'A_2 P', P'A_3 P'),$$

which by Remark 2.3 (a) and (b) is the joint numerical range of three hermitian $s \times s$ matrices. If p lies outside W' , then p is a corner point of W . Otherwise, $p \in W'$ leads to a contradiction, because $W' = W$ has no one-dimensional nonexposed faces. Indeed, if $s = 3$, then every nonexposed face of W' is a nonexposed point by [59, Lemma 4.3]. The convex set W' has no nonexposed faces at all if $s = 2$ (where W' is a linear image of a three-dimensional Euclidean ball) or if $s = 1$ (where W' is a singleton). \square

The following proposition highlights a special property of 4×4 matrices, whose analogue fails for the 5×5 matrices in Example 5.3 above.

Proposition 5.6. *Suppose a one-dimensional nonexposed face F_2 of W intersects a one-dimensional exposed face G of W . Let p be the extreme point of W such that $F_2 \cap G = \{p\}$. Then p is a corner point of W or G is contained in the unique non-elliptic face of W that includes F_2 .*

Proof. The face F_2 is an exposed face of a non-elliptic face F_1 . Thus, the assumptions of Lemma 5.4 are fulfilled and we use its results and notation.

Zooming in onto the exposed face G , we use a unitary 4×4 matrix U such that the projection Q associated to G is unitarily similar to $\mathbf{1}_2 \oplus 0 = UQU^*$. Then by Remark 2.3 (b), the hermitian 2×2 matrices $B_i := (UA_i U^*)[2]$, $i = 1, 2, 3$, are such that

$$G = W(B_1, B_2, B_3).$$

As Q is the kernel projection of A_2 , the first two columns of U^* may be taken as the unit vectors $(1, 0, 0, 0)^\top$ and $(0, z_1, z_2, z_3)^\top$. Hence

$$B_1 = \begin{bmatrix} 0 & 0 \\ 0 & |z_3|^2 \end{bmatrix} \quad \text{and} \quad B_3 = \begin{bmatrix} 0 & z_3 w_1 \\ \bar{z}_3 \bar{w}_1 & * \end{bmatrix}.$$

If $z_3 = 0$, then $Q \leq P_1$ implies $G \subset F_1$ as desired. Otherwise, if $z_3 \neq 0$, then we invoke the fact that G is a segment. This implies that B_1 and B_3 commute. Then $w_1 = 0$ follows and it implies $A_1, A_2, A_3 \in 0 \oplus M_3$. Now Lemma 5.5 shows that $p = (0, 0, 0)^\top$ is a corner point of W . \square

Remark 5.7. The optimality of Proposition 5.6 can be seen from examples.

- (a) The first disjunct of the disjunctive assertion of Proposition 5.6 fails for the joint numerical range W in Example E7a. This numerical range has two faces H_1, H_2 of droplet shapes. The segment $G_0 := H_1 \cap H_2$ is an exposed face of W and the other boundary segment G_1 of H_1 is a nonexposed face of W . As G_0 and G_1 intersect at a nonexposed points, this point cannot be a corner point.
- (b) The second disjunct fails for certain joint numerical ranges W having one face of droplet shape. Let W' be the three-dimensional joint numerical range of three hermitian 3×3 matrices, such that W' has exactly one face of elliptic shape, say E , but W' is not a pyramid based on E , see [59, Example 6.2]. Let W be the convex hull of W' and a point p in the affine hull of E but outside W' . The convex hull H of p and E is a face of W of droplet shape, whose two boundary segments G_1, G_2 are nonexposed faces of W . Still, W has a whole family of one-dimensional exposed faces containing p that are not included in H .
- (c) The assertion of Proposition 5.6 cannot be strengthened to an exclusive disjunction. This can be seen from Example E7b (or E9). This numerical range has two faces H_1, H_2 of droplet shapes. The segment $G_0 := H_1 \cap H_2$ is an exposed face of W . The boundary segment G_i of H_i that differs from G_0 is a nonexposed face of W , $i = 1, 2$, and the segments G_0, G_1, G_2 intersect at a point p . Theorem 5.10 shows that p is a corner point of W , thereby proving the first disjunct. As G_0 is included in the unique non-elliptic face H_1 that includes G_1 , the second disjunct is also true.
- (d) Matrices of higher order (i.e. $n \geq 5$) are excluded from the statement of Proposition 5.6 by Example 5.3.

Proposition 5.8. *Suppose G_1, G_2 are distinct one-dimensional nonexposed faces of W that are included in distinct non-elliptic faces of W , and let G be a one-dimensional exposed face of W . Suppose $G_1 \cap G_2 \cap G \neq \emptyset$. Then $G_1 \cap G_2 \cap G = \{p\}$ is a corner point of W .*

Proof. Let H_i denote the non-elliptic face including G_i , $i = 1, 2$. If G is not included in H_1 , then p is a corner point of W by Proposition 5.6.

Let $G \subset H_1$. We use results and notation from Lemma 5.4 assuming $F_1 := H_1$ and $F_2 := G_1$. The projection associated to H_1 is the kernel projection P_1 of $A_1 = \text{diag}(0, 0, 0, 1)$. The projection associated to G is the kernel projection Q of A_2 , which is a positive semidefinite matrix of rank two, and which simplifies (because of $G \subset H_1$) to

$$A_2 = 0 \oplus \begin{bmatrix} |\psi\rangle\langle\psi| & z|\psi\rangle \\ \bar{z}\langle\psi| & a \end{bmatrix},$$

where $|\psi\rangle \in \mathbb{C}^2$ is a unit vector, $a > 0$, and $z \in \mathbb{C}$ satisfies $|z| < \sqrt{a}$.

One easily finds that the projection R associated to H_2 is the kernel projection of

$$A := A_2 - \lambda A_1 = 0 \oplus \begin{bmatrix} |\psi\rangle\langle\psi| & z|\psi\rangle \\ \bar{z}\langle\psi| & |z|^2 \end{bmatrix},$$

where $\lambda = a - |z|^2$ is chosen so $A_2 - \lambda A_1$ becomes a positive semidefinite matrix of rank one.

Similarly to Proposition 5.6, we use a unitary 4×4 matrix U such that R is unitarily similar to $\mathbb{1}_3 \oplus 0 = URU^*$. Then the hermitian 3×3 matrices $B_i := (UA_iU^*)[3]$, $i = 1, 2, 3$, yield

$$H_2 = W(B_1, B_2, B_3).$$

Taking the first three columns of U^* as the orthonormal vectors

$$\begin{aligned} |1\rangle &:= (1, 0, 0, 0)^\top, \\ |2\rangle &:= 0 \oplus |\psi^\perp\rangle \oplus 0, \\ |3\rangle &:= (0 \oplus (-z)|\psi\rangle \oplus 1) / \sqrt{1 + |z|^2}, \end{aligned}$$

where $|\psi^\perp\rangle \in \mathbb{C}^2$ is a unit vector orthogonal to $|\psi\rangle$, one has

$$B_1 = \begin{bmatrix} 0 & 0 & 0 \\ 0 & * & * \\ 0 & * & * \end{bmatrix}, \quad B_2 = \begin{bmatrix} 0 & 0 & 0 \\ 0 & * & * \\ 0 & * & * \end{bmatrix}, \quad B_3 = \frac{1}{\sqrt{1 + |z|^2}} \begin{bmatrix} 0 & 0 & w_1 \\ 0 & * & * \\ w_1 & * & * \end{bmatrix}.$$

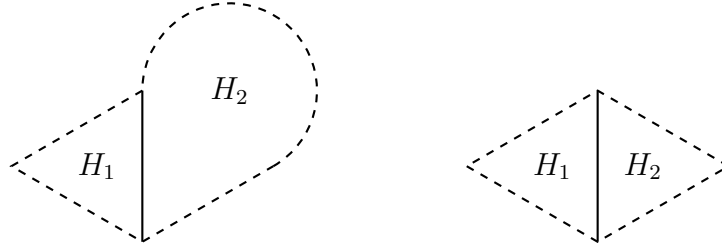
Finally, the assumption that G and G_2 intersect at $p = (0, 0, 0)^\top$ takes effect. It shows that p is a corner point of H_2 . Therefore, $B_1, B_2, B_3 \in 0 \oplus M_2$ holds by Proposition 2.5, which implies $w_1 = 0$, hence $A_1, A_2, A_3 \in 0 \oplus M_3$. Now Lemma 5.5 shows that p is a corner point of W . \square

Lemma 5.9. *The intersection of any three mutually distinct one-dimensional non-exposed faces of W is empty.*

Proof. Let G_1, G_2, G_3 be mutually distinct one-dimensional nonexposed faces of W and let H_i denote the non-elliptic face of W that includes G_i , $i = 1, 2, 3$. We distinguish three cases.

First, if $H_1 = H_2 = H_3$ then H_1 is a triangle and the intersection $G_1 \cap G_2 \cap G_3$ of its three sides is empty.

Second, if exactly two of H_1, H_2, H_3 are equal, say $H_1 \neq H_2 = H_3$, then by Lemma 3.1, $S := H_1 \cap H_2$ is a one-dimensional face of H_1 and of H_2 , and an exposed face of W . As the G_i 's are faces of H_1 and of H_2 , too, the number of one-dimensional faces of H_i , summed over $i = 1, 2$, is at least five (two for S counted twice plus three for the G_i 's). This forces one of the H_i 's, say H_1 , to be a triangle and the other, say H_2 , to be a droplet or a triangle. In either case, see the following figure, we have $G_1 \cap G_2 \cap G_3 = \emptyset$.



Third, let H_1, H_2, H_3 be mutually distinct. Then $S_1 := H_2 \cap H_3$, $S_2 := H_3 \cap H_1$, and $S_3 := H_1 \cap H_2$ are mutually distinct one-dimensional exposed face of W by Lemma 3.1 and Lemma 3.4. The numbers of one-dimensional faces of H_i , summed over $i = 1, 2, 3$, yield at least nine (six for the S_i 's counted twice plus three for the G_i 's). This proves that each of the H_i 's is a triangle. Now Lemma 3.5 shows that W is a tetrahedron, which has no nonexposed faces, a contradiction. \square

Theorem 5.10. *If the intersection of three mutually distinct one-dimensional faces of W is nonempty, then this intersection is a corner point of W .*

Proof. Let G_1, G_2, G_3 denote the one-dimensional faces in question. Then $G_1 \cap G_2 \cap G_3 = \{p\}$ where p is an extreme point of W (this is the statement of Remark 5.1 (b)).

By Lemma 5.2 and Lemma 5.9, the claim is true unless exactly two of the faces G_1, G_2, G_3 are nonexposed.

Let G_1, G_2 be one-dimensional nonexposed faces, let H_i be the non-elliptic face including G_i , $i = 1, 2$, and let G_3 be a one-dimensional exposed face of W . First, let $H_1 = H_2$. If $G_3 \subset H_1$, then H_1 is a triangle and the intersection $G_1 \cap G_2 \cap G_3$ of its three sides is empty. Since $G_3 \subset H_1$ fails, Proposition 5.6 shows that p is a corner point of W . Second, if $H_1 \neq H_2$ then p is a corner point of W by Proposition 5.8. \square

6. On elliptic faces

Let A_1, A_2, A_3 be hermitian 4×4 matrices. We collect observations on elliptic faces of the joint numerical range $W = W(A_1, A_2, A_3)$. We assume $\dim(W) = 3$.

Lemma 6.1. *If an elliptic face of W differs from a rank-3 face of W , then their intersection is an exposed point of W , and hence an exposed point of that rank-3 face.*

Proof. Let F be a face of W that is an ellipse and let G be a rank-3 face. Let P (resp., Q) denote the projection associated to F (resp., G) in Theorem 2.1. Then P has rank two or three and Q has rank three. Hence the intersection of the ranges of P and Q is at least one-dimensional, and consequently the faces F and G have a non-empty intersection.

Since F and G have dimension two, they are exposed faces of W and so is their intersection. As F is an ellipse, this intersection is a singleton, hence an exposed point of W . *A fortiori*, this point is an exposed point of G . \square

Remark 6.2. In view of Lemma 6.1, one may ask whether an elliptic face of W can intersect the endpoints of a one-dimensional face of a non-elliptic face. This is impossible for a type-1 non-elliptic face (loaf), as the endpoints of its one-dimensional face are nonexposed points.

An elliptic face of W can intersect the vertex of a non-elliptic droplet face. An example is the joint numerical range (see Figure 6.1 (a)) of the matrices

$$\begin{bmatrix} 0 & 1 \\ 1 & 0 \end{bmatrix} \oplus \begin{bmatrix} 1 & 0 \\ 0 & 1 \end{bmatrix}, \begin{bmatrix} 0 & -i \\ i & 0 \end{bmatrix} \oplus \begin{bmatrix} 0 & 1 \\ 1 & 0 \end{bmatrix}, \begin{bmatrix} -2 & 0 \\ 0 & -2 \end{bmatrix} \oplus \begin{bmatrix} 0 & -i \\ i & 0 \end{bmatrix},$$

which is the convex hull of the unit circle in the x - y -plane translated by -2 in z -direction and the unit circle in the y - z -plane translated by 1 in x -direction.

An elliptic face of W can also intersect the vertex of a triangular face. An example is the joint numerical range (see Figure 6.1 (b)) of the matrices

$$\begin{bmatrix} 0 & 1 \\ 1 & 0 \end{bmatrix} \oplus \begin{bmatrix} 1 & 0 \\ 0 & -1 \end{bmatrix}, \begin{bmatrix} 0 & -i \\ i & 0 \end{bmatrix} \oplus \begin{bmatrix} 0 & 0 \\ 0 & 0 \end{bmatrix}, \begin{bmatrix} 0 & 0 \\ 0 & 0 \end{bmatrix} \oplus \begin{bmatrix} 1 & 0 \\ 0 & 1 \end{bmatrix},$$

which is the convex hull of the unit circle in the x - y -plane and the points $(1, 0, 1)^\top$, $(-1, 0, 1)^\top$.

To put this paper into a broader context, we quote the work [47] by Ottem et al. and we sketch a proof as to why their results imply that $W = W(A_1, A_2, A_3)$ has generically an even number of at most ten faces of rank two that are elliptic discs and no other faces of rank two or three, provided that A_1, A_2, A_3 are real symmetric 4×4 matrices.

Remark 6.3 (Generic faces are ellipses). Given real symmetric 4×4 matrices $\tilde{A}_0, \tilde{A}_1, \tilde{A}_2, \tilde{A}_3$, the authors of [47] define a complex projective *symmetroid*

$$\tilde{V} = \{(u_0 : u_1 : u_2 : u_3) \in \mathbb{C}\mathbb{P}^3 : \det(u_0\tilde{A}_0 + u_1\tilde{A}_1 + u_2\tilde{A}_2 + u_3\tilde{A}_3) = 0\}$$

and a real projective *spectrahedron*

$$\tilde{S} = \{(u_0 : u_1 : u_2 : u_3) \in \mathbb{R}\mathbb{P}^3 : u_0\tilde{A}_0 + u_1\tilde{A}_1 + u_2\tilde{A}_2 + u_3\tilde{A}_3 \geq 0\}.$$

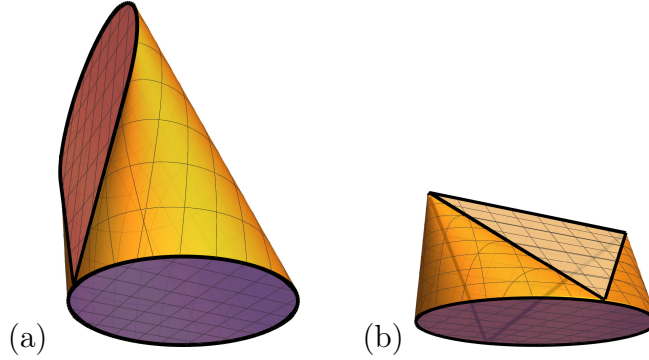


Figure 6.1: The joint numerical ranges showing adjacency of elliptic faces and exposed points of non-elliptic ones.

They assume $\dim \tilde{S} = 3$, which implies that the linear span of $\tilde{A}_0, \tilde{A}_1, \tilde{A}_2, \tilde{A}_3$ contains a positive definite matrix. Hence, a real projectivity transforms the symmetroid \tilde{V} to the symmetroid

$$V := \{(u_0 : u_1 : u_2 : u_3) \in \mathbb{C}\mathbb{P}^3 : \det(u_0 \mathbb{1}_4 + u_1 A_1 + u_2 A_2 + u_3 A_3) = 0\}$$

and the spectrahedron \tilde{S} to the spectrahedron

$$S := \{(u_0 : u_1 : u_2 : u_3) \in \mathbb{R}\mathbb{P}^3 : u_0 \mathbb{1}_4 + u_1 A_1 + u_2 A_2 + u_3 A_3 \geq 0\},$$

where A_1, A_2, A_3 are linearly independent real symmetric 4×4 matrices of trace zero. It follows that S does not intersect the hyperplane $u_0 = 0$ at infinity and so S is a compact convex subset of the affine space $\mathbb{R}^3 \cong \{u_0 = 1\}$ that has a well-known geometry [46].

Ottem et al. [47] restrict their analysis to *transversal symmetroids* \tilde{V} and *transversal spectrahedra* \tilde{S} , which means that \tilde{V} has exactly ten points of (matrix) rank two and no other points of rank smaller than three (singular points). The symmetroid \tilde{V} is transversal for all quadruples $(\tilde{A}_0, \tilde{A}_1, \tilde{A}_2, \tilde{A}_3)$ in the complement of an algebraic set that is strictly included in the set of all quadruples of real symmetric 4×4 matrices. The singularities are characterized by tangent cones: If zero is in \tilde{V} in an affine chart of $\mathbb{C}\mathbb{P}^3$, then the *tangent cone* of \tilde{V} at zero is the lowest degree part of $\det(u_0 \tilde{A}_0 + u_1 \tilde{A}_1 + u_2 \tilde{A}_2 + u_3 \tilde{A}_3)$ in that chart. The tangent cone at a point of rank two is thus a quadratic cone. We have the following equivalence:

- (i) the point $u_0 \mathbb{1}_4 + u_1 A_1 + u_2 A_2 + u_3 A_3$ has rank two, (6.1)
- (ii) the tangent cone of V at $u_0 \mathbb{1}_4 + u_1 A_1 + u_2 A_2 + u_3 A_3$ is a quadratic cone.

It is shown in [47], Theorem 1.1, that an even number σ of the ten points of rank two of \tilde{V} are contained in \tilde{S} , provided that \tilde{V} is transversal.

Since $W = \{x \in \mathbb{R}^3 : \forall u \in S, 1 + \langle x, u \rangle \geq 0\}$ is the *dual convex set* to S , see [51, Corollary 5.3], and since the origin $0 \in \mathbb{R}^3$ is an interior point of the compact convex

set S , it follows that every exposed face of W is the intersection of the Euclidean boundary ∂W of W with the normal cone $N_S(u)$ of S at some point $u \in S$, see [63, Section 8]. The *dual convex cone* $\{v \in \mathbb{R}^3 : \forall x \in N_S(u), \langle x, v \rangle \geq 0\}$ to the normal cone $N_S(u)$ is the *support cone* $T_S(u)$, which is defined as the Euclidean closure of the convex cone $\bigcup_{\lambda > 0} \lambda(S - u)$, see [55, Section 2.2]. Thus, up to a translation along u , the Euclidean boundary $\partial T_S(u)$ of $T_S(u)$ is the set of points on the rays that are limits of rays emanating from u that intersect ∂S in points that converge to u . This implies that the *algebraic boundary* of $T_S(u)$, which is the smallest complex projective algebraic set that contains $\partial T_S(u)$, is the tangent cone of the symmetroid V at u , see [57, Section 2.1.5]. Thus, the assertions in (6.1) are equivalent to each of the following ones if $u = (u_1, u_2, u_2)^\top \in S$ are the coordinates of a point in $\mathbb{R}^3 \cong \{u_0 = 1\}$.

- (iii) the support cone $T_S(u)$ is an elliptic convex cone, (6.2)
- (iv) the normal cone $N_S(u)$ is an elliptic convex cone,
- (v) the face $N_S(u) \cap \partial W$ of W is an ellipse.

The preceding two paragraphs show that $W(A_1, A_2, A_3)$ has an even number $\sigma \leq 10$ of rank-two faces that are elliptic disks and no other faces of rank two or three, provided that S is a transversal spectrahedron. This is the case for all (A_1, A_2, A_3) in the complement of an algebraic set that is strictly included in the set of all triples of real symmetric 4×4 matrices. In particular, it is true for all triples in an open and dense subset in the Euclidean topology.

To clarify what we mean by obtaining $(\mathbb{1}_4, A_1, A_2, A_3)$ from $\tilde{A}_0, \tilde{A}_1, \tilde{A}_2, \tilde{A}_3$ through a real projectivity in Remark 6.3 above, we assume for simplicity that $A := \tilde{A}_0 + \tilde{A}_1 + \tilde{A}_2 + \tilde{A}_3$ is positive definite. Then the projectivity $(u_0 : u_1 : u_2 : u_3) \mapsto (u_0 : u_1 - u_0 : u_2 - u_0 : u_3 - u_0)$ maps \tilde{V} to

$$\begin{aligned} & \{(u_0 : u_1 : u_2 : u_3) \in \mathbb{C}\mathbb{P}^3 : \det(u_0 A + u_1 \tilde{A}_1 + u_2 \tilde{A}_2 + u_3 \tilde{A}_3) = 0\} \\ & = \{(u_0 : u_1 : u_2 : u_3) \in \mathbb{C}\mathbb{P}^3 : \det(u_0 \mathbb{1}_4 + u_1 A_1 + u_2 A_2 + u_3 A_3) = 0\}, \end{aligned}$$

where $A_i := A^{-\frac{1}{2}} \tilde{A}_i A^{-\frac{1}{2}}$, $i = 1, 2, 3$. Further projectivities allow us to replace A_1, A_2, A_3 with traceless matrices. The matrix A is indeed positive definite and the symmetroid \tilde{V} is transversal in the examples in [47, Section 2]. For these examples $W(A_1, A_2, A_3)$ has an even number $\sigma \leq 10$ of rank-2 faces that are elliptic disks and no other faces of rank two or three.

One of the important results of [47] is that every transversal spectrahedron S has an even number $\sigma \leq 10$ of points of rank two and no other points of rank smaller than three. By Remark 6.3, this can be interpreted by saying that the joint numerical range $W(A_1, A_2, A_3)$ dual to S has an even number $\sigma \leq 10$ of rank-2 faces that are elliptic disks and no other faces of rank two and three. However, we found joint numerical ranges with 1, 3, 5 elliptic faces — this is possible because

the dual spectrahedra are not transversal, as some elliptical faces are of rank three. Similarly, the spectrahedra dual to the Examples E1–E14 in Section 4 above cannot be transversal.

Consider the joint numerical range with five elliptic faces (shown in Figure 6.2 (a)), obtained for the following three matrices:

$$\begin{bmatrix} 0 & 0 & 1 & 0 \\ 0 & 0 & 0 & 0 \\ 1 & 0 & 0 & 0 \\ 0 & 0 & 0 & 0 \end{bmatrix}, \begin{bmatrix} 0 & 0 & 0 & 0 \\ 0 & 0 & 0 & 1 \\ 0 & 0 & 0 & 0 \\ 0 & 1 & 0 & 0 \end{bmatrix}, \begin{bmatrix} 1 & 0 & 0 & 0 \\ 0 & 0 & 1 & 0 \\ 0 & 1 & 0 & 0 \\ 0 & 0 & 0 & 1 \end{bmatrix}$$

In this case the relevant spectrahedron is not transversal, since the top elliptic face is of rank 3, and can be regarded as an affine linear image of the numerical range $W(B_1, B_2)$ of the following matrices:

$$B_1 = \begin{bmatrix} 0 & 0 & 1 \\ 0 & 0 & 0 \\ 1 & 0 & 0 \end{bmatrix}, \quad B_2 = \begin{bmatrix} 0 & 1 & 0 \\ 1 & 0 & 0 \\ 0 & 0 & 0 \end{bmatrix}.$$

This illustrates Remark 3.2: these are bordered matrices, resulting in elliptic numerical range.

Without the exact knowledge of the projectors onto subspaces associated with the elliptic faces, it is not possible to determine whether or not they intersect: simple reasoning based on dimension counting like in Lemma 3.1 are indecisive. Compare the following two examples with the same structure of subspaces dimensions: each of the matrices in both examples has two double eigenvalues of -1 and $+1$, but there are significant differences in geometry of the joint numerical ranges.

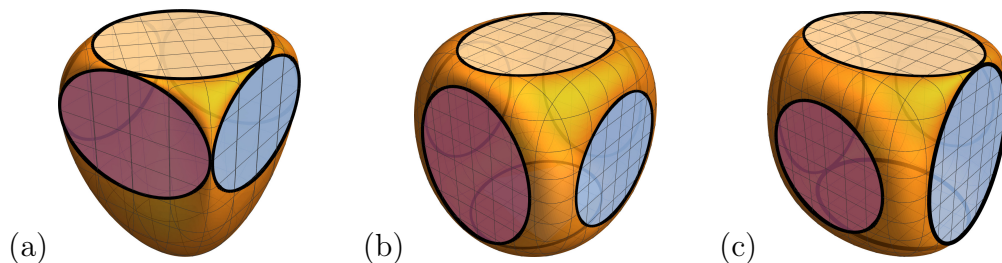


Figure 6.2: Examples of joint numerical ranges for triples of 4×4 hermitian matrices with various configurations of elliptic faces: (a) five faces, (b) six non-adjacent, (c) six with two disjoint from the remaining four.

One of joint numerical ranges forms a ‘dice’ and contains six elliptic faces, which are pairwise disjoint (see Figure 6.2 (b)), and is obtained for the following matrices:

$$\frac{1}{\sqrt{2}} \begin{bmatrix} 1 & 1 & 0 & 0 \\ 1 & -1 & 0 & 0 \\ 0 & 0 & -1 & 1 \\ 0 & 0 & 1 & 1 \end{bmatrix}, \begin{bmatrix} 0 & -1 & 0 & 0 \\ -1 & 0 & 0 & 0 \\ 0 & 0 & 0 & 1 \\ 0 & 0 & 1 & 0 \end{bmatrix}, \begin{bmatrix} 0 & 0 & 0 & -1 \\ 0 & 0 & i & 0 \\ 0 & -i & 0 & 0 \\ -1 & 0 & 0 & 0 \end{bmatrix}.$$

A joint numerical range with six elliptic faces, four of them intersecting in a ring pattern, and two disjoint (see Figure 6.2 (c)), corresponds to the following triple of symmetric matrices:

$$\frac{1}{\sqrt{2}} \begin{bmatrix} 1 & 1 & 0 & 0 \\ 1 & -1 & 0 & 0 \\ 0 & 0 & -1 & 1 \\ 0 & 0 & 1 & 1 \end{bmatrix}, \begin{bmatrix} 0 & -1 & 0 & 0 \\ -1 & 0 & 0 & 0 \\ 0 & 0 & 0 & 1 \\ 0 & 0 & 1 & 0 \end{bmatrix}, \begin{bmatrix} 0 & 0 & 0 & -1 \\ 0 & 0 & 1 & 0 \\ 0 & 1 & 0 & 0 \\ -1 & 0 & 0 & 0 \end{bmatrix}.$$

7. Separable numerical range

Some applications in quantum physics rely on the notion of *restricted numerical range*, in which the set of states \mathcal{D}_A is replaced with a specific subset [21]. In the case of systems composed of two parts – e.g., two qubits – this subset might correspond to states which are in some sense classical, and the numerical range restricted to such states highlights the difference between classical and quantum behaviors of quantum systems.

Let us start with the mathematical description of the physical scenario. If the physical operations and observable quantities of the first system are described by the set M_d of matrices of size d (forming a $*$ -algebra on \mathbb{C}^d), and the operations and observables on the second subsystem by $M_{d'}$ (analogously, a $*$ -algebra on $\mathbb{C}^{d'}$), the total physical bipartite (two-party) system corresponds to the tensor product of algebras. As in Section 2 above, we denote the set of density matrices of size d by \mathcal{D}_d . With this notation, the density matrices of the entire system can be denoted by $\mathcal{D}_{d \times d'}$: they are positive semidefinite, unit trace matrices of order $d \cdot d'$. Here, we mostly concentrate on two-qubit systems, as this matches the topic of this paper: two qubits correspond to the state space \mathcal{D}_4 needed in the definition of joint numerical ranges for matrices of size four.

One of the most interesting features of such a description is that some states give rise to correlations that can not be explained by classical probability theory. In some sense, the "classical" nature of some states is captured by the fact that they can be decomposed into a convex sum of tensor products of one-subsystem states – such states are called *separable* [34]:

$$\mathcal{D}_{d \times d'}^{\text{sep}} = \text{conv}\{ \rho^A \otimes \rho^B : \rho^A \in \mathcal{D}_d, \rho^B \in \mathcal{D}_{d'} \}. \quad (7.1)$$

Here we study the *separable states of two qubits* $\mathcal{D}_{2 \times 2}^{\text{sep}}$, as this is a proper subset of \mathcal{D}_4 , projections of which are the main topic of this article. By analogy to the definition of joint numerical range (see (2.3)), we define the *separable numerical range* [21]

$$W^{\text{sep}}(A_1, \dots, A_k) = w(\mathcal{D}_{d \times d'}^{\text{sep}}) = \{ (\text{tr } \rho A_1, \dots, \text{tr } \rho A_k) : \rho \in \mathcal{D}_{d \times d'}^{\text{sep}} \}. \quad (7.2)$$

The object defined in such a way (as well as the related product numerical range, where only rank one product states are taken into account, leading to nonconvexity

[52]), are important tools in quantum information theory, allowing for the study of quantum entanglement [58]. In practice, the tensor product, which is a central point to the study of entanglement, is typically realized as the Kronecker product. Temporarily employing the physical notation of $|0\rangle = (1, 0)^\top \in \mathbb{C}^2$ and $|1\rangle = (0, 1)^\top \in \mathbb{C}^2$, the Kronecker products $|ij\rangle = |i\rangle \otimes |j\rangle$ of the two vectors take the following form:

$$|00\rangle = \begin{pmatrix} 1 \\ 0 \\ 0 \\ 0 \end{pmatrix}, \quad |01\rangle = \begin{pmatrix} 0 \\ 1 \\ 0 \\ 0 \end{pmatrix}, \quad |10\rangle = \begin{pmatrix} 0 \\ 0 \\ 1 \\ 0 \end{pmatrix}, \quad \text{and} \quad |11\rangle = \begin{pmatrix} 0 \\ 0 \\ 0 \\ 1 \end{pmatrix}.$$

Similarly, the tensor product appearing in (7.1) is here interpreted as

$$\begin{pmatrix} A_{11} & A_{12} \\ A_{21} & A_{22} \end{pmatrix} \otimes \overbrace{\begin{pmatrix} B_{11} & B_{12} \\ B_{21} & B_{22} \end{pmatrix}}^B = \begin{pmatrix} A_{11}B & A_{12}B \\ A_{21}B & A_{22}B \end{pmatrix}.$$

Physical motivation here is to characterize the difference between entangled and separable states through the associated numerical ranges – with this in mind, we analyze the question: how the shape of the boundary ∂W of the standard joint numerical range of three hermitian matrices of order four, investigated in previous sections, influences the structure of the corresponding separable numerical range W^{sep} .

The particular case of two-qubit system is not difficult to probe numerically through the use of semidefinite optimization due to the positive partial transpose (PPT) criterion [50, 34]:

Theorem 7.1 (Peres-Horodeccy). *For $(d, d') = (2, 2)$ and $(2, 3)$, the states belonging to $\mathcal{D}_{d,d'}^{\text{sep}}$ are characterised by semidefinite positivity of their partial transpose:*

$$\rho \in \mathcal{D}_{d \times d'}^{\text{sep}} \Leftrightarrow \rho \in \mathcal{D}_{d \times d'} \text{ and } \rho^\Gamma \in \mathcal{D}_{d \times d'},$$

where \cdot^Γ denotes the partial transpose. For the matrix $X \in \mathbb{M}_{2 \times d}$ of square blocks $\{Y, Z, U, V\}$ of size d

$$X = \begin{pmatrix} Y & Z \\ U & V \end{pmatrix},$$

the partial transpose is the transpose of each of the blocks:

$$X^\Gamma = \begin{pmatrix} Y^\top & Z^\top \\ U^\top & V^\top \end{pmatrix}$$

This condition can be used together with semidefinite optimization in order to determine exposed faces of W^{sep} , allowing for numerical study and visualisations of the set. In what follows, we consider two qubits, where $(d, d') = (2, 2)$ and A_1, A_2, A_3 are hermitian matrices of order four.

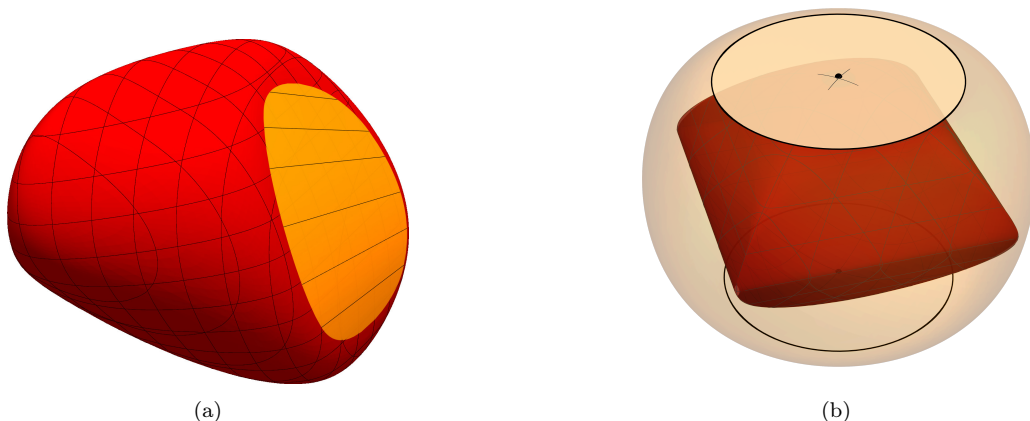


Figure 7.1: (a) Separable numerical range (red) for randomly sampled matrices (7.4); according to Remark 7.3, the boundary contains a ruled surface (yellow region) some of whose lines are depicted. (b) Joint and separable numerical ranges (transparent yellow and solid red, respectively) for the matrices (7.5) illustrate Lemma 7.4: the two circular faces of the joint numerical range (at the top and bottom) intersect the separable numerical range (black dots).

Lemma 7.2. *Let F be an exposed face of $W^{\text{sep}}(A_1, A_2, A_3)$ minimizing the linear functional $W^{\text{sep}} \ni p \mapsto \sum_{i=1}^3 s_i p_i$. The preimage of F under the measure map given by (2.1) is characterized as the solutions to the following semidefinite optimization problem:*

$$\min_{\rho} \text{tr} \rho \left(\sum_{i=1}^k A_i s_i \right) \tag{7.3}$$

subject to $\rho \geq 0$, $\rho^{\Gamma} \geq 0$, $\text{tr} \rho = 1$.

Proof. If a point $p \in W^{\text{sep}}$, there must exist a hermitian matrix ρ of order four such that $w(\rho) = p$, and by Theorem 7.1 it must fulfill $\text{tr} \rho = 1$, $\rho \geq 0$ and $\rho^{\Gamma} \geq 0$. If $p \in F$, for any other $\sigma \in \mathcal{D}_{2 \times 2}^{\text{sep}}$, $\sum_{i=1}^3 s_i \text{tr}(\rho A_i) \leq \sum_{i=1}^3 s_i \text{tr}(\sigma A_i)$, and therefore ρ is a solution to the semidefinite optimization problem (7.3). \square

For visualisation purposes it is sufficient to sample the functional parameters (n_1, n_2, n_3) from the unit sphere S_2 , and for each numerically determine an optimizer ρ to the above minimization problem. If the optimization converges, the point $w(\rho)$ lies at the boundary of the separable numerical range, within prescribed optimization accuracy (which is well controlled for semidefinite problems [43]). Then, the convex hull of the sampled boundary points approximates $W^{\text{sep}}(A_1, A_2, A_3)$.

To the best of our knowledge, this approximation procedure is the only way of studying the separable numerical ranges, if the matrices do not possess any additional structure. The numerically probed geometry of three-dimensional W^{sep} always seems to contain singular features⁷.

⁷This is in contrast with two-dimensional separable numerical ranges, which for generic matrices

Remark 7.3 (Numerical empirical finding). For hermitian matrices A_1, A_2, A_3 sampled i.i.d. from the Gaussian Unitary Ensemble of matrices of size 4, the boundary of the separable numerical range $W^{\text{sep}}(A_1, A_2, A_3)$ always contains singular elements: cusps, flat faces, or ruled surfaces. Right now it is only a numerical observation, as we are not aware of any techniques to prove that singular features do exist in this case.

We attribute this observation to possible construction of W^{sep} as a convex hull of the analogous product numerical range [52],

$$W^{\text{sep}} = \text{conv } W^{\otimes}, \text{ with } W^{\otimes} = w_{A_1, A_2, A_3}(\{\rho \in \mathcal{D}^{\text{sep}} : \text{rk } \rho = 1\}).$$

The set W^{\otimes} appears to be nonconvex under the assumptions of the above Remark, and ruled surfaces form in W^{sep} as a result of this. An example of the above observation is provided in Figure 7.1a. There, the ruled surface of the separable numerical range is highlighted; the matrices are taken from the Gaussian Unitary Ensemble and approximated by rational coefficients for reproducibility:

$$\begin{bmatrix} -3 & -9 - 6i & -15 - i & -2 + 13i \\ * & 6 & -2 + 5i & -2 + 10i \\ * & * & -10 & -6 - 7i \\ * & * & * & 3 \end{bmatrix}, \begin{bmatrix} 11 & 9 + 2i & 2 - 5i & -1 - 2i \\ * & -9 & -4 - 3i & 1 - 4i \\ * & * & -16 & 10 - 12i \\ * & * & * & -2 \end{bmatrix}, \quad (7.4)$$

$$\begin{bmatrix} 15 & 10 - 3i & 5 + 5i & -i \\ * & -6 & -16 - 2i & 15 \\ * & * & 3 & -9 - 7i \\ * & * & * & -13 \end{bmatrix}$$

Numerically, the ruled surfaces do not seem to be caused by the rational structure of coefficients. Their existence is a generic behavior. Practically, the matrices were generated in Mathematica 14.1 with the following code.

```
SeedRandom[2137];
10 Round[ RandomVariate[GaussianUnitaryMatrixDistribution[4], 3], 1/10]
```

The separable numerical range must lie within the joint numerical range, as separable states form a subset of all states. The two ranges can be tangent to each other, and this is known to happen if the joint numerical range has a face that is not a point.

Lemma 7.4. *Every rank-2 and rank-3 face of the joint numerical range $W(A_1, A_2, A_3)$ intersects the separable numerical range $W^{\text{sep}}(A_1, A_2, A_3)$. In particular, every face of $W(A_1, A_2, A_3)$ that is larger than a singleton intersects $W^{\text{sep}}(A_1, A_2, A_3)$.*

do not contain any boundary segments. Note that due to the numerical approximation procedure, the decision whether a given region of the boundary is flat is somewhat arbitrary; here we take the ruled surfaces to be the regions with large segments between the vertices of the convex hull, which persist despite subsampling.

Proof. Every rank-2 or rank-3 face is an image (under w) of a subset S of \mathcal{D}_4 isomorphic with \mathcal{D}_2 or \mathcal{D}_3 , respectively, by Theorem 2.1. In particular, this is true for every face that is larger than a singleton.

This set S is the convex hull of the rank-one projectors onto vectors belonging to a 2- or 3-dimensional subspace of \mathbb{C}^4 . It is known that any 2-dimensional subspace of \mathbb{C}^4 contains a pure tensor $v_A \otimes v_B$ (see [54, Theorem 2]). So the projector Π onto $v_A \otimes v_B$ is contained in $S \cap \mathcal{D}_{2 \times 2}^{\text{sep}}$ and $w(v_A \otimes v_B)$ is contained in $W^{\text{sep}}(A_1, A_2, A_3)$. \square

Lemma 7.4 is illustrated in Figure 7.1b for the following matrices.

$$\begin{bmatrix} 0 & 1 & 0 & 1 \\ * & 0 & 1 & 0 \\ * & * & 0 & 0 \\ * & * & * & 0 \end{bmatrix}, \quad \begin{bmatrix} 0 & -i & 0 & i \\ * & 0 & -i & 0 \\ * & * & 0 & 0 \\ * & * & * & 0 \end{bmatrix}, \quad \text{diag}(-1, 1, 1, -1) \quad (7.5)$$

Acknowledgments

SW thanks Cynthia Vinzant for helpful discussions on convex duality and on the results of [47]. KS gratefully acknowledges funding from the projects DeQHOST APVV-22-0570, QUAS VEGA 2/0164/25, Postdokgrant APD0161, and Stefan Schwarz programme. SW was supported by the European Union under the project ROBO-PROX (reg. no. CZ.02.01.01/00/22_008/0004590), while KŽ acknowledges support under ERC Advanced Grant Tatypic, Project No. 101142236.

References

- [1] M. Adam, J. Maroulas, *The joint numerical range of bordered and tridiagonal matrices*, in I. Gohberg, H. Langer (eds.), *Linear Operators and Matrices*, Oper. Theory: Adv. Appl. vol. 130, Basel: Birkhäuser, 2002, 29–41.
- [2] E.M. Alfsen, F.W. Shultz, *State Spaces of Operator Algebras: Basic Theory, Orientations, and C^* -products*, Boston: Birkhäuser, 2001.
- [3] W. Arveson, *The noncommutative Choquet boundary III*, *Mathematica Scandinavica* 106:2, 196–210 (2010).
- [4] H. Aslaksen, A.B. Sletsjøe, *Generators of matrix algebras in dimension 2 and 3*, *Lin. Algebra Appl.* **430**, 1–6 (2009).
- [5] Y.-H. Au-Yeung, Y.-T. Poon, *A remark on the convexity and positive definiteness concerning hermitian matrices*, *Southeast Asian Bull. Math.* 3:2, 85–92 (1979).
- [6] N. Bebiano, J. da Providência, I. Spitkovsky, K. Vazquez, *Kippenhahn curves of some tridiagonal matrices*, *Filomat* 35:9, 3047–3061 (2021).

- [7] I. Bengtsson, K. Życzkowski, *Geometry of Quantum States: An Introduction to Quantum Entanglement*, 2nd ed., Cambridge: Cambridge University Press, 2017.
- [8] P. Binding, C.-K. Li, *Joint ranges of hermitian matrices and simultaneous diagonalization*, *Lin. Algebra Appl.* **151**, 157–167 (1991).
- [9] F. F. Bonsall, J. Duncan, *Numerical Ranges of Operators on Normed Spaces and of Elements of Normed Algebras*, London: Cambridge University Press, 1971.
- [10] O. Bratteli, D. W. Robinson, *Operator Algebras and Quantum Statistical Mechanics 1*, Berlin: Springer, 1987.
- [11] E. S. Brown, I. M. Spitkovsky, *On matrices with elliptical numerical ranges*, *Linear and Multilinear Algebra* 52:3–4, 177–193 (2004).
- [12] M.-T. Chien, H. Nakazato, *Joint numerical range and its generating hypersurface*, *Lin. Algebra Appl.* **432**, 173–179 (2010).
- [13] M.-D. Choi, E. G. Effros, *Injectivity and operator spaces*, *Journal of Functional Analysis* 24:2, 156–209 (1977).
- [14] I. Csiszár, F. Matúš, *Closures of exponential families*, *The Annals of Probability* 33:2, 582–600 (2005).
- [15] L. E. Dickson, *Algebraic Theories*, New York: Dover Publications, 1959.
- [16] C. F. Dunkl, P. Gawron, J. A. Holbrook, J. MiszczaK, Z. Puchała, K. Życzkowski, *Numerical shadow and geometry of quantum states*, *J. Phys. A* **44** 335301 (19pp) (2011).
- [17] D. R. Farenick, *Algebras of Linear Transformations*, New York: Springer, 2001.
- [18] M. Fiedler, *Geometry of the numerical range of matrices*, *Lin. Algebra Appl.* **37**, 81–96 (1981).
- [19] G. Fischer, *Plane Algebraic Curves*, Providence: AMS, 2001.
- [20] H.-L. Gau, P. Y. Wu, *Numerical Ranges of Hilbert Space Operators*, 1st ed., Cambridge University Press, 2021.
- [21] P. Gawron, Z. Puchała, J. A. MiszczaK, Ł. Skowronek, K. Życzkowski, *Restricted numerical range: a versatile tool in the theory of quantum information*, *J. Math. Phys.* **51** 102204 (24pp) (2010).
- [22] B. Grünbaum, *Convex Polytopes*, 2nd ed., New York: Springer, 2003.
- [23] K. E. Gustafson, D. K. M. Rao, *Numerical range: The Field of Values of Linear Operators and Matrices*, New York: Springer, 1997.

- [24] E. Gutkin, *The Toeplitz-Hausdorff theorem revisited: Relating linear algebra and geometry*, The Mathematical Intelligencer 26:1, 8–14 (2004).
- [25] E. Gutkin, E. A. Jonckheere, M. Karow, *Convexity of the joint numerical range: topological and differential geometric viewpoints*, Lin. Algebra Appl. **376**, 143–171 (2004).
- [26] E. Gutkin, K. Życzkowski, *Joint numerical ranges, quantum maps, and joint numerical shadows*, Lin. Algebra Appl. **438**, 2394–2404 (2013).
- [27] K. H. Han, S.-H. Kye, *Supporting hyperplanes for Schmidt numbers and Schmidt number witnesses*, Open Syst. Inf. Dyn. 32:02, 2550008 (2025).
- [28] F. Hausdorff, *Der Wertvorrat einer Bilinearform*, Mathematische Zeitschrift 3:1, 314–316 (1919).
- [29] T. Heinosaari, L. Mazzarella, M. M. Wolf, *Quantum tomography under prior information*, Communications in Mathematical Physics 318:2, 355–374 (2013).
- [30] M. Helsø, K. Ranestad, *Rational quartic spectrahedra*, Math. Scand. 127:1, 79–99 (2021).
- [31] R. A. Horn, C. R. Johnson, *Matrix Analysis*, 2nd ed., New York: Cambridge University Press, 2012.
- [32] R. A. Horn, C. R. Johnson, *Topics in Matrix Analysis*, Cambridge: Cambridge Univ. Press, 1991.
- [33] R. A. Horn, F. Zhang, *Basic Properties of the Schur Complement*, in: F. Zhang (ed.), *The Schur Complement and Its Applications*, New York: Springer, 2005.
- [34] M. Horodecki, P. Horodecki, R. Horodecki, *Separability of mixed states: necessary and sufficient conditions*, Physics Letters A 223 (1996)
- [35] S. Jevtic, M. Pusey, D. Jennings, T. Rudolph, *Quantum steering ellipsoids*, Physical Review Letters 113 (2014)
- [36] D. S. Keeler, L. Rodman, and I. M. Spitkovsky, *The numerical range of 3×3 matrices*, Lin. Algebra Appl. **252**, 115–139 (1997).
- [37] R. Kippenhahn, *Über den Wertevorrat einer Matrix*, Mathematische Nachrichten 6:3–4, 193–228 (1951).
- [38] D.W. Kribs, A. Pasieka, M. Laforest, C. Ryan, M.P. da Silva, *Research problems on numerical ranges in quantum computing*, Linear and Multilinear Algebra **57**, 491-502 (2009).

- [39] C.-K. Li, Y.-T. Poon, Y.-S. Wang, *Joint numerical ranges and commutativity of matrices*, J. Math. Anal. Appl. **491** 124310, (2020).
- [40] R. Liss, T. Mor, A. Winter, *Geometry of entanglement and separability in Hilbert subspaces of dimension up to three*, Lett. Math Phys. 114:86 (2024).
- [41] R. Loewy, B.-S. Tam, *Complementation in the face lattice of a proper cone*, Lin. Algebra Appl. **79**, 195–207 (1986).
- [42] B. Maier, T. Netzer, *A note on the Carathéodory number of the joint numerical range*. J. Convex Anal. 33 (2026), no. 1–2, 517–519.
- [43] M. Michałek, B. Sturmfels, *Invitation to Nonlinear Algebra*, Graduate Studies in Mathematics, Vol. 211, AMS, 2021.
- [44] S. Morelli, C. Eltschka, M. Huber, J. Siewert, *Correlation constraints and the Bloch geometry of two qubits*, Phys. Rev. A 109:1, 012423 (2024).
- [45] V. Müller, Yu. Tomilov, *Joint numerical ranges: recent advances and applications minicourse by V. Müller and Yu. Tomilov*, Concrete Operators 7:1, 133–154 (2020).
- [46] T. Netzer, D. Plaumann, *Geometry of Linear Matrix Inequalities: A Course in Convexity and Real Algebraic Geometry with a View Towards Optimization*, Cham: Springer, 2023.
- [47] J. C. Ottem, K. Ranestad, B. Sturmfels, C. Vinzant, *Quartic spectrahedra*, Mathematical Programming, 151:2, 585–612 (2015).
- [48] V.I. Paulsen, *Completely Bounded Maps and Operator Algebras*, New York: Cambridge University Press, 2003.
- [49] V.I. Paulsen, S. Severini, D. Stahlke, I.G. Todorov, A. Winter, *Estimating quantum chromatic numbers*, Journal of Functional Analysis 270:6, 2188–2222 (2016).
- [50] A. Peres, *Separability criterion for density matrices*, Physical Review Letters 77 (1996).
- [51] D. Plaumann, R. Sinn, S. Weis, *Kippenhahn’s theorem for joint numerical ranges and quantum states*, SIAM J. Appl. Algebra Geometry 5:1, 86–113 (2021).
- [52] Z. Puchała, P. Gawron, J.A. Miszczak, Ł. Skowronek, M.-D. Choi, K. Życzkowski, *Product numerical range in a space with tensor product structure*, Lin. Algebra Appl. **434**, 327–342 (2011).
- [53] R. T. Rockafellar, *Convex Analysis*, Princeton: Princeton University Press, 1970.

- [54] A. Sanpera, R. Tarrach, G. Vidal, *Local description of quantum inseparability*, Physical Review A 58, 826 (1998).
- [55] R. Schneider, *Convex Bodies: The Brunn-Minkowski Theory*, 2nd ed., New York: Cambridge University Press, 2014.
- [56] T. Schulte-Herbrüggen, G. Dirr, U. Helmke, S. J. Glaser, *The significance of the C -numerical range and the local C -numerical range in quantum control and quantum information*, Linear and Multilinear Algebra 56:1–2, 3–26 (2008).
- [57] I. R. Shafarevich, *Basic Algebraic Geometry 1*, Berlin: Springer, 2013.
- [58] T. Simnacher, J. Czartowski, K. Szymański, K. Życzkowski, *Confident entanglement detection via separable numerical range*, Phys. Rev. A **104**, 042420 (2021).
- [59] K. Szymański, S. Weis, K. Życzkowski, *Classification of joint numerical ranges of three hermitian matrices of size three*, Lin. Algebra Appl. **545**, 148–173 (2018).
- [60] O. Toeplitz, *Das algebraische Analogon zu einem Satze von Fejér*, Mathematische Zeitschrift 2:1–2, 187–197 (1918).
- [61] S. Weis, *Quantum convex support*, Lin. Algebra Appl. **435**, 3168–3188 (2011). Erratum, LAA 436:1, xvi (2012).
- [62] S. Weis, *A note on touching cones and faces*, Journal of Convex Analysis 19:2, 323–353 (2012).
- [63] S. Weis, *Information topologies on non-commutative state spaces*, Journal of Convex Analysis 21:2, 339–399 (2014).
- [64] S. Weis, *A variational principle for ground spaces*, Reports on Mathematical Physics 82:3, 317–336 (2018).
- [65] R.F. Werner, *Quantum states with Einstein-Podolsky-Rosen correlations admitting a hidden-variable model*, Physical Review A 40, 4277–4281 (1989).
- [66] J. Xie et al., *Observing Geometry of Quantum States in a Three-Level System*, Physical Review Letters 125, 150401 (2020)